Master's Thesis

석사 학위논문

An Enhanced Time-Delay Control using a Second-Order Time-Delay Estimation for Robot Manipulators

Jin Ho Do (도 진 호 都 珍 鎬)

Department of Robotics Engineering

로봇공학전공

DGIST

2013

Master's Thesis
석사 학위논문

An Enhanced Time-Delay Control using a Second-Order Time-Delay Estimation for Robot Manipulators

Jin Ho Do (도 진 호 都 珍 鎬)

Department of Robotics Engineering
로봇공학전공

DGIST

2013

An Enhanced Time-Delay Control using a Second-Order Time-Delay Estimation for Robot Manipulators

Advisor   : Professor   Pyung Hun Chang

Co-advisor : Professor   Jeon Il Moon

by

Jin Ho Do

Department of Robotics Engineering

DGIST

A thesis submitted to the faculty of DGIST in partial fulfillment of the requirements for the degree of Master of Science in the Department of Robotics Engineering. The study was conducted in accordance with Code of Research Ethics[1].

May. 15. 2013

Approved by

Professor   Pyung Hun Chang   (Signature)

(Advisor)

Professor   Jeon Il Moon   (Signature)

(Co-advisor)

---

1) Declaration of Ethical Conduct in Research: I, as a graduate student of DGIST, hereby declare that I have not committed any acts that may damage the credibility of my research. These include, but are not limited to: falsification, thesis written by someone else, distortion of research findings or plagiarism. I affirm that my thesis contains honest conclusions based on my own careful research under the guidance of my thesis advisor.

An Enhanced Time-Delay Control using a
Second-Order Time-Delay Estimation
for Robot Manipulators

Jin Ho Do

Accepted in partial fulfillment of the requirements for the degree of
Master of Science.

May. 15. 2013

Head of Committee   Prof. Pyung Hun Chang   (인)

Committee Member   Prof. Jeon Il Moon   (인)

Committee Member   Prof. Jae Sung Hong   (인)

ABSTRACT

In this thesis, I present analysis of Time-Delay Control (TDC) and Enhanced Time-Delay Control (ETDC) for robot manipulators. Each control will be analyzed and represented by their characteristics. In addition, a new controller with combining strong points from each control scheme will be proposed.

Time-Delay Control is a well-known controller because it is simple and robust, but it has a problem; Time Delay Estimation (TDE) errors occur because the TDC uses TDE scheme to estimate uncertainties of robot manipulators with discontinuous dynamics, also known as hard nonlinearities.

In order to remedy the problem, ETDC is proposed. While it compensates for the TDE error, a new problem is created: chattering. In order to alleviate the problem, a new controller, which is much more robust than ETDC is proposed. It also shows better initial error than ETDC. Simulations and experimentations show the effectiveness of the proposed controller.

Contents

Ⅰ. Introduction

Ⅱ. Literature Study

Ⅲ. Design and Analysis of Proposed Control

IV . Simulation

V . Experimentation

VI . Conclusion

List of tables

List of figures

(a) desired trajectory (b) desired velocity

(a) Tracking error at joint 6 (b) velocity error at joint 6 (c) torque at joint 6

(a) tracking error at joint 6 (b) velocity error at joint 6 (c) torque at joint 6

(a) desired trajectory (b) desired velocity

(a) tracking error with various characteristic gains

(b) torque with various characteristic gains

(a) desired trajectory (b) desired velocity

(a) tracking error at joint 1 (b) tracking error at joint 2 (c) tracking error at joint 3

(d) tracking error at joint 4 (e) tracking error at joint 5 (f) tracking error at joint 6

(a) torque at joint 1 (b) torque at joint 2 (c) torque at joint 3

(d) torque at joint 4 (e) torque at joint 5 (f) torque at joint 6

(a) tracking error at joint 1 (b) tracking error at joint 2 (c) tracking error at joint 3

(d) tracking error at joint 4 (e) tracking error at joint 5 (f) tracking error at joint 6

Ⅰ. Introduction

1.1 Research background and motivations

Robust Control techniques are one of several control schemes used to control plants with modeling errors or model uncertainty to follow desired dynamic behavior. Mathematical models of robot manipulators include model uncertainty because of friction, backlash, and varying loads with respect to time. Therefore, a highly complicated controller is needed to control the motion of robot manipulators accurately. However, implementation of a complicated controller is inefficient because of it being difficult to design and heavy computational requirements.

A complicated controller is both difficult to design and heavy computational burdens make implementation inefficient. Hence, a robust controller with a simple structure and easy design is needed.

One type of robust controller is Time Delay Control (TDC) [3] for robot manipulators. TDC uses Time

Delay Estimation (TDE) to estimate the uncertainty of models such as disturbances and unknown dynamics. TDC also has a simple structure in addition to computational efficiency [4, 5, 6, 12]. TDC for robot manipulators has been successfully applied [3, 12, 7, 8, 11], and demonstrated to be useful and effective.

TDC for robot manipulators estimates the Coriolis effect, centrifugal effect, and gravitational effect by using previous input, output, and certain diagonal matrix for moment of inertia [4, 5, 6, 12]. Small amounts of information are needed to estimate nonlinear terms in TDC for robot manipulators. Accordingly, TDC for robot manipulators has little computational burden. However, the control performance of TDC is degraded when plants have, what is known as hard nonlinearity such as static friction and Coulomb friction. Hard nonlinearity has faster dynamics characteristics than time delayed information in TDC [14, 15, 9, 17]. In particular, plants with static friction and Stribeck show Stick-Slip phenomena when TDC is applied to the plants. Also, when the velocity of joints is at zero, plants with Coulomb friction show performance degradation. In order to secure good performance, new schemes must be created to compensate for the above phenomena.

Time Delay Control with Switching Action (TDCSA) research tried to compensate for the above phenomena in TDC, [15, 9]. TDCSA combines TDC with concept of Sliding Mode Control (SMC) as a compensator. TDCSA shows enhanced performance over TDC because SMC inputs appropriate values into plant in a discontinuous manner. TDCSA has been successfully applied to excavator [16] and proved to be useful. However, TDCSA has chattering problems because of the discontinuous input. Furthermore, two parameters in TDCSA need to be tuned to give properly compensated input.

Other researches like Time Delay Control with Internal Model Concept (TDCIM) [17] and Enhanced Time Delay Control (ETDC) [1] emerged. TDCIM combines TDC and concept of Internal Model. TDCIM shows enhanced performance over TDC because the feed-back of internal model concept in TDCIM adds to TDC. Consequently, TDCIM has a structure with double integral and also has little computational burden. However, the stability of TDCIM is lower than TDC because of the double feed-back in TDCIM. ETDC combines TDC and TDE error term. ETDC shows better performance than TDC because of the TDE error term in ETDC [1]. The TDE error term in ETDC cancels the TDE error. ETDC does not need additional gain in additional TDE error term and also has little computational

burden like the TDCIM. But, ETDC shows high frequency noise like chattering [Appendix A].

Consequently, ETDC needs additional filters to reduce the noise like chattering.

In this thesis, new control scheme is proposed to remedy the problem in ETDC. The new solution

contains TDE error term like ETDC and this term combines a certain gain. So, the characteristics of

the new controller can be changed by tuning the gain. Consequently, the new controller does not

need additional filters like ETDC and shows enhanced performance found in ETDC.

1.2 Composition of thesis synopsis

Chapter 1 describes background of the research and purpose. Chapter 2 will describe the

preliminaries necessary for this research, including Time Delay Control (TDC) and Enhanced Time

Delay Control (ETDC). Chapter 3 will represent the design method of the proposed controller. It will

be analyzed in frequency response with ETDC and TDC. Chapter 4 and 5 will present simulations

and experimentations to prove implementation of the proposed control and performance. Finally,

Chapter 6 will summarize the findings of the paper and state the conclusion.

Ⅱ. Literature Study

2.1 Time Delay control

2.1.1 Outline

Time Delay Control (TDC) uses Time Delay Estimation (TDE) scheme to estimate unknown

dynamics, disturbances, Coriolis effect, and the like in plants. The structure of TDC is very simple

because of the TDE scheme. In addition, TDC needs small amounts of information in terms of the

plant. Because of these advantages, TDC has been applied to various fields [3, 4, 5, 12, 8].

However, the control performance of TDC degrades when plants include what is known as hard

nonlinearity, such as static friction and Coulomb friction. This is because the hard nonlinearity has

faster dynamics characteristic than time delayed information in TDC [14, 15, 9, 17]. Particularly, plants

with effects of static friction and Stribeck show Stick-Slip phenomena in steady state by integral term

of TDC when TDC is applied in plants. Also, when the velocity of joints is at zero, plants with Coulomb friction show degraded performance.

In this thesis, TDC is analyzed to find the causes of above phenomena. Therefore, TDC investigation is briefly noted in 2.1.2. In 2.1.3, causes of the phenomena in TDC are analyzed with TDE error.

2.1.2 Time Delay Control

In MORGAN's research in 1985, TDE scheme is used to measure disturbance [10]. TDC law of general linear or nonlinear system is derived from K. Youcef-Toumi [4, 5]. TDC law based on Proportional Differential (PD) control for robot manipulators is derived from T. C. Hsia around the same time [12, 13].

The general dynamics of robot manipulators can be described as follows:

$$\mathbf{M}(\boldsymbol{\theta})\ddot{\boldsymbol{\theta}} + \mathbf{V}(\boldsymbol{\theta}, \dot{\boldsymbol{\theta}}) + \mathbf{G}(\boldsymbol{\theta}) + \mathbf{F}(\boldsymbol{\theta}, \dot{\boldsymbol{\theta}}) = \boldsymbol{\tau} \tag{2.1}$$

Where $\mathbf{M}(\boldsymbol{\theta})$ denotes $n \times n$ inertia matrix, n is the number of joints in robot manipulators, $\boldsymbol{\theta}$ is the vector of a joint variable of $n \times 1$, $\mathbf{V}(\boldsymbol{\theta}, \dot{\boldsymbol{\theta}})$ is Coriolis force and centrifugal force of vector of $n \times 1$,

$\mathbf{G(\theta)}$ is gravity vector of $n \times 1$, $\mathbf{F(\theta, \dot{\theta})}$ is a certain force like friction and disturbance, and $\mathbf{\tau}$ is torque

of $n \times 1$ vector applying to the joint.

In (2.1), $\mathbf{\bar{M}}$ is adopted instead of $\mathbf{M(\theta)}$. $\mathbf{\bar{M}}$ is a constant matrix and based on $\mathbf{M(\theta)}$. Then, the

equation (2.1) can be described as follows:

$$\mathbf{\bar{M}\ddot{\theta} + H(\theta, \dot{\theta}, \ddot{\theta}) = \tau} \tag{2.2}$$

When nonlinear vector $\mathbf{H(\theta, \dot{\theta}, \ddot{\theta})}$ includes entire nonlinear terms, disturbance, and other factors in

robot manipulators, then, $\mathbf{H(\theta, \dot{\theta}, \ddot{\theta})}$ can be described as follows:

$$\mathbf{H(\theta, \dot{\theta}, \ddot{\theta}) = (M(\theta) - \bar{M})\ddot{\theta} + V(\theta, \dot{\theta}) + G(\theta) + F(\theta, \dot{\theta})} \tag{2.3}$$

By using Computed Torque Control scheme, $\mathbf{\tau}$ can be described as follows:

$$\mathbf{\tau = \bar{M}u + \hat{H}} \tag{2.4}$$

$$\mathbf{u = \ddot{\theta}_d + K_D(\dot{\theta}_d - \dot{\theta}) + K_P(\theta_d - \theta)} \tag{2.5}$$

Where $\mathbf{\hat{H}}$ is estimation value of $\mathbf{H}$. $\mathbf{K_D}$ and $\mathbf{K_P}$ are $n \times n$ diagonal matrix of Proportional

Differential (PD) gain. If $\mathbf{\hat{H} = H}$ is valid, relationship between $\mathbf{\ddot{\theta}}$ and $\mathbf{u}$ is valid from equation (2.2)

and (2.4) as follows:

$$\ddot{\boldsymbol{\theta}} = \mathbf{u} \tag{2.6}$$

Equation (2.5) applies to (2.6). Then, error dynamics of closed loop of TDC can be described as follows:

$$\ddot{\mathbf{e}} + \mathbf{K_D}\dot{\mathbf{e}} + \mathbf{K_P}\mathbf{e} = 0 \tag{2.7}$$

Where, $\mathbf{e} \triangleq \boldsymbol{\theta_d} - \boldsymbol{\theta}$.

To find estimation value of nonlinear vector $\mathbf{H}$, TDC uses Time Delay Estimation(TDE) scheme. If time delay L has a tiny value, approximation equation is valid from equation (2.2) as follows:

$$\mathbf{H}_{(t)} \cong \hat{\mathbf{H}}_{(t)}$$

$$= \mathbf{H}_{(t-L)} = \boldsymbol{\tau}_{(t-L)} - \bar{\mathbf{M}}\ddot{\boldsymbol{\theta}}_{(t-L)} \tag{2.8}$$

Equation (2.5) and (2.8) apply to (2.4). Then, TDC raw can be described as follows:

$$\boldsymbol{\tau} = \boldsymbol{\tau}_{(t-L)} - \bar{\mathbf{M}}\ddot{\boldsymbol{\theta}}_{(t-L)}$$

$$+\bar{\mathbf{M}}\big[\ddot{\boldsymbol{\theta}}_{\mathbf{d}} + \mathbf{K_D}\big(\dot{\boldsymbol{\theta}}_{\mathbf{d}} - \dot{\boldsymbol{\theta}}\big) + \mathbf{K_P}(\boldsymbol{\theta}_{\mathbf{d}} - \boldsymbol{\theta})\big] \tag{2.9}$$

If $\bar{\mathbf{M}}$ is selected as a diagonal constant matrix, TDC is independent joint controller with PD gain and

$\bar{\mathbf{M}}$. Then, TDC block diagram can be described simply in figure 2.1. In other words, by using TDE

scheme, TDC does not compute complicated nonlinear dynamics. Advantages of TDC are its

efficiency and has light burden in terms of computation.
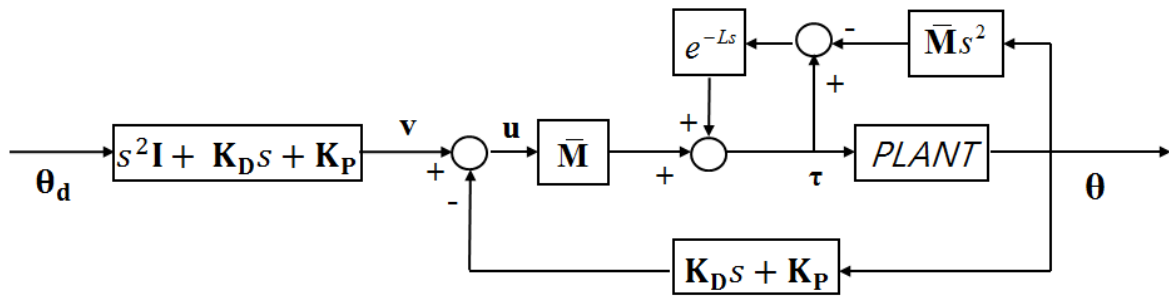
Fig. 2.1 TDC Block Diagram

Robustness of TDC in closed loop systems is determined by precise TDE value in terms of

nonlinearity, un-modeled dynamics, disturbance, and other factors. In the efficiency of TDE scheme,

time delay L is very important. In a manner of speaking as qualitative, time delay L should be selected

with an assumption that $\mathbf{H}_{(t)}$ is continuous, to remain valid. Namely, time delay L should be tiny value

as much as possible to estimate the information well.

2.1.3 Time Delay Estimation Error

Generally, TDC can have error dynamics like equation (2.7) when time delay *L* has sufficiently tiny value. However, time delay *L* cannot actually be zero in real-world systems. When TDC is applied to real-world systems, time delay *L* is generally used as sampling time. Time delay *L* is limited to be close to zero because of hardware limitations. So, TDE error can be occurred from time delay *L*, which is not zero because of hardware limitations in real-world systems. The relationship can be induced from equation (2.2), (2.4), and (2.8) as follows:

$$\bar{\mathbf{M}}\left(\mathbf{u}_{(t)} - \ddot{\boldsymbol{\theta}}_{(t)}\right) = \mathbf{H}_{(t)} - \widehat{\mathbf{H}}_{(t)}$$

$$= \mathbf{H}_{(t)} - \mathbf{H}_{(t-L)} \tag{2.10}$$

In equation (2.10), right side term represents TDE error. Then, TDE error can be defined as follows:

$$\Delta\mathbf{H}_{(t)} \triangleq \bar{\mathbf{M}}\left(\mathbf{u}_{(t)} - \ddot{\boldsymbol{\theta}}_{(t)}\right) = \mathbf{H}_{(t)} - \widehat{\mathbf{H}}_{(t)} = \mathbf{H}_{(t)} - \mathbf{H}_{(t-L)} \tag{2.11}$$

When a TDE error occurs, the error dynamics of TDE cannot be described as shown in equation (2.7). The error dynamics can be described from equation (2.5) and (2.11) as follows:

$$\ddot{\mathbf{e}} + \mathbf{K_D}\dot{\mathbf{e}} + \mathbf{K_P}\mathbf{e} = \bar{\mathbf{M}}^{-1}\Delta\mathbf{H}_{(t)} \tag{2.12}$$

A TDE error can be ignored for the most part when the time delay L is sufficiently smaller than dynamic characteristics of nonlinearities and disturbance in systems. However, plants have very fast dynamic characteristics like static friction, Coulomb friction, and others. It is difficult to accurately estimate above information because of above reasons. Therefore, it is possible for TDE errors to increase and as a result large tracking error can occur when TDC is applied to systems with static and Coulomb friction.

2.2 Enhanced Time Delay Control

2.2.1 Outline

Time Delay Control (TDC) can estimate uncertainties of plants by using Time Delay Estimation (TDE) scheme. However, control performance of TDC is degraded by TDE errors. Hence, an advanced research, Enhanced Time Delay Control (ETDC) was developed by J. Y. Park and P. H. Chang in 2003 [1]. ETDC are more accurate than TDC at the same sampling frequency. Also, ETDC has nearly the same computational efficiency as TDC. In 2.2.2, ETDC raw is described and difference

points between TDC and ETDC is represented. In 2.2.3, TDE error term in ETDC is derived as

different form and analyzed in terms of fundamental significance. In 2.2.4, error dynamics of ETDC is

derived and analyzed in terms of frequency response.

2.2.2 Enhanced Time Delay Control

ETDC adds approximated TDE errors into TDC to compensate for TDE errors. Then, TDC

with approximated TDE error is described (2.4) as follows:

$$\boldsymbol{\tau} = \bar{\mathbf{M}}\mathbf{u} + \hat{\mathbf{H}}_{\mathbf{ETDC}} \tag{2.13}$$

$$\hat{\mathbf{H}}_{\mathbf{ETDC}} = \hat{\mathbf{H}} + \overline{\Delta\mathbf{H}} \tag{2.14}$$

Where $\overline{\Delta\mathbf{H}}$ is the approximated TDE errors. $\mathbf{u}$ is equal to the equation (2.5). $\hat{\mathbf{H}}$ is also equal to the

equation (2.8).

To find approximated TDE errors, the main concept of ETDC states TDE error at the present time t

can be approximated by TDE error at the previous time *t-L* if the time delay *L* is sufficiently small. The

approximated TDE error can be described from (2.2) and (2.11) as follows:

$$\overline{\Delta\mathbf{H}}_{(t)} \cong \Delta\mathbf{H}_{(t-L)}$$

$$= \mathbf{H}_{(t-L)} - \mathbf{H}_{(t-2L)} = \left(\boldsymbol{\tau}_{(t-L)} - \overline{\mathbf{M}}\ddot{\boldsymbol{\theta}}_{(t-L)}\right) - \left(\boldsymbol{\tau}_{(t-2L)} - \overline{\mathbf{M}}\ddot{\boldsymbol{\theta}}_{(t-2L)}\right) \qquad (2.15)$$

Equation (2.15) applies to (2.14). Then, estimation of $\mathbf{H}$ in ETDC can be described as follows:

$$\widehat{\mathbf{H}}_{\mathbf{ETDC}} = \widehat{\mathbf{H}}_{(t)} + \Delta\mathbf{H}_{(t-L)} \qquad (2.16)$$

From equation (2.5), (2.11), (2.13), and (2.16), error dynamics of ETDC can be described as follows:

$$\ddot{\mathbf{e}} + \mathbf{K_D}\dot{\mathbf{e}} + \mathbf{K_P}\mathbf{e} = \overline{\mathbf{M}}^{-1}(\Delta\mathbf{H}_{(t)} - \Delta\mathbf{H}_{(t-L)}) \qquad (2.17)$$

If time delay *L* is sufficiently small, TDE error at present time *t* can be compensated by TDE error at

previous time *t-L*. Then, the error dynamics of ETDC can be the same as equation (2.7).

From equation (2.5), (2.13), and (2.16), ETDC raw can be described as follows:

$$\boldsymbol{\tau} = \overline{\mathbf{M}}\left[\ddot{\boldsymbol{\theta}}_{\mathbf{d}} + \mathbf{K_D}\left(\dot{\boldsymbol{\theta}}_{\mathbf{d}} - \dot{\boldsymbol{\theta}}\right) + \mathbf{K_P}(\boldsymbol{\theta}_{\mathbf{d}} - \boldsymbol{\theta})\right] + \widehat{\mathbf{H}}_{(t)} + \Delta\mathbf{H}_{(t-L)} \qquad (2.18)$$

Rearranging equation (2.18) with (2.15), ETDC raw can be described again as follows:

$$\boldsymbol{\tau} = 2\left(\boldsymbol{\tau}_{(t-L)} - \overline{\mathbf{M}}\ddot{\boldsymbol{\theta}}_{(t-L)}\right) - \left(\boldsymbol{\tau}_{(t-2L)} - \overline{\mathbf{M}}\ddot{\boldsymbol{\theta}}_{(t-2L)}\right)$$

$$+ \overline{\mathbf{M}}\left[\ddot{\boldsymbol{\theta}}_{\mathbf{d}} + \mathbf{K_D}\left(\dot{\boldsymbol{\theta}}_{\mathbf{d}} - \dot{\boldsymbol{\theta}}\right) + \mathbf{K_P}(\boldsymbol{\theta}_{\mathbf{d}} - \boldsymbol{\theta})\right] \qquad (2.19)$$

In error dynamics of TDC and ETDC (2.12) and (2.17), if TDE error is very slowly changed, TDE

error can be ignored. Then, the error dynamics of both is equal to zero as shown in equation (2.7).

However, if term of $\mathbf{H}$ changes too fast, TDC cannot cancel the TDE error. Consequently, as can be

seen from (2.12), TDC cannot track the desired dynamics accurately. In such a situation, ETDC

shows better performance of control than TDC, Since TDE errors can be compensated by TDE errors

at previous time.

2.2.3 Time Delay Estimation Error Term

TDE error term in ETDC consists of torque, inertia matrix, and angular acceleration. In the

TDE error term (2 .15), $\boldsymbol{\tau}_{(t-L)}$ is also computed by the controller in previous time: *t-L*. The $\boldsymbol{\tau}_{(t-L)}$ is

computed by using equation (2.19) used *t-L* instead of *t* as follows:

$$\boldsymbol{\tau}_{(t-L)} = 2\big(\boldsymbol{\tau}_{(t-2L)} - \overline{\mathbf{M}}\ddot{\boldsymbol{\theta}}_{(t-2L)}\big) - \big(\boldsymbol{\tau}_{(t-3L)} - \overline{\mathbf{M}}\ddot{\boldsymbol{\theta}}_{(t-3L)}\big)$$

$$+\overline{\mathbf{M}}\big[\ddot{\boldsymbol{\theta}}_{\mathbf{d}(t-L)} + \mathbf{K_D}\big(\dot{\boldsymbol{\theta}}_{\mathbf{d}(t-L)} - \dot{\boldsymbol{\theta}}_{(t-L)}\big) + \mathbf{K_P}\big(\boldsymbol{\theta}_{\mathbf{d}(t-L)} - \boldsymbol{\theta}_{(t-L)}\big)\big] \qquad (2.20)$$

Equation (2.15) is described with (2.20) as follows:

$$\Delta \mathbf{H}_{(t-L)} = \overline{\mathbf{M}}\big[\big(\ddot{\boldsymbol{\theta}}_{\mathbf{d}(t-L)} - \ddot{\boldsymbol{\theta}}_{(t-L)}\big) + \mathbf{K_D}\big(\dot{\boldsymbol{\theta}}_{\mathbf{d}(t-L)} - \dot{\boldsymbol{\theta}}_{(t-L)}\big) + \mathbf{K_P}\big(\boldsymbol{\theta}_{\mathbf{d}(t-L)} - \boldsymbol{\theta}_{(t-L)}\big)\big]$$

$$+\big(\boldsymbol{\tau}_{(t-2L)} - \overline{\mathbf{M}}\ddot{\boldsymbol{\theta}}_{(t-2L)}\big) - \big(\boldsymbol{\tau}_{(t-3L)} - \overline{\mathbf{M}}\ddot{\boldsymbol{\theta}}_{(t-3L)}\big) \qquad (2.21)$$

In equation (2.21), $\big(\boldsymbol{\tau}_{(t-2L)} - \overline{\mathbf{M}}\ddot{\boldsymbol{\theta}}_{(t-2L)}\big) - \big(\boldsymbol{\tau}_{(t-3L)} - \overline{\mathbf{M}}\ddot{\boldsymbol{\theta}}_{(t-3L)}\big)$ is TDE error term (2.15) with *t-L*

instead of *t.* Then, equation (2.21) is described as follows:

$$\Delta \mathbf{H}_{(t-L)} = \overline{\mathbf{M}}\big[\big(\ddot{\boldsymbol{\theta}}_{\mathbf{d}(t-L)} - \ddot{\boldsymbol{\theta}}_{(t-L)}\big) + \mathbf{K_D}\big(\dot{\boldsymbol{\theta}}_{\mathbf{d}(t-L)} - \dot{\boldsymbol{\theta}}_{(t-L)}\big) + \mathbf{K_P}\big(\boldsymbol{\theta}_{\mathbf{d}(t-L)} - \boldsymbol{\theta}_{(t-L)}\big)\big] + \Delta \mathbf{H}_{(t-2L)} \quad (2.22)$$

From (2.22), TDE error term contains previous TDE error. Therefore, TDE error term can be

described by using previous TDE error terms as follows:

$$\Delta \mathbf{H}_{(t-L)} = \overline{\mathbf{M}}\big[\big(\ddot{\boldsymbol{\theta}}_{\mathbf{d}(t-L)} - \ddot{\boldsymbol{\theta}}_{(t-L)}\big) + \mathbf{K_D}\big(\dot{\boldsymbol{\theta}}_{\mathbf{d}(t-L)} - \dot{\boldsymbol{\theta}}_{(t-L)}\big) + \mathbf{K_P}\big(\boldsymbol{\theta}_{\mathbf{d}(t-L)} - \boldsymbol{\theta}_{(t-L)}\big)\big]$$

$$+\overline{\mathbf{M}}\big[\big(\ddot{\boldsymbol{\theta}}_{\mathbf{d}(t-2L)} - \ddot{\boldsymbol{\theta}}_{(t-2L)}\big) + \mathbf{K_D}\big(\dot{\boldsymbol{\theta}}_{\mathbf{d}(t-2L)} - \dot{\boldsymbol{\theta}}_{(t-2L)}\big) + \mathbf{K_P}\big(\boldsymbol{\theta}_{\mathbf{d}(t-2L)} - \boldsymbol{\theta}_{(t-2L)}\big)\big]$$

$$\bullet\bullet\bullet$$

$$+\overline{\mathbf{M}}\big[\big(\ddot{\boldsymbol{\theta}}_{\mathbf{d}(t-kL)} - \ddot{\boldsymbol{\theta}}_{(t-kL)}\big) + \mathbf{K_D}\big(\dot{\boldsymbol{\theta}}_{\mathbf{d}(t-kL)} - \dot{\boldsymbol{\theta}}_{(t-kL)}\big) + \mathbf{K_P}\big(\boldsymbol{\theta}_{\mathbf{d}(t-kL)} - \boldsymbol{\theta}_{(t-kL)}\big)\big] \qquad (2.23)$$

Where k is operation count, time t defines operation counts and sampling time: $t \triangleq kL.$

From equation (2.23), TDE error term in ETDC accumulated $\overline{\mathbf{M}}\big[\big(\ddot{\boldsymbol{\theta}}_{\mathbf{d}(t)} - \ddot{\boldsymbol{\theta}}_{(t)}\big) + \mathbf{K_D}\big(\dot{\boldsymbol{\theta}}_{\mathbf{d}(t)} - \dot{\boldsymbol{\theta}}_{(t)}\big) +$

$\mathbf{K_P}\big(\boldsymbol{\theta}_{\mathbf{d}(t)} - \boldsymbol{\theta}_{(t)}\big)\big]$ term from *t-L* to initial time.

ETDC raw can be described in time domain with TDE error (2.22) as follows:

$$\boldsymbol{\tau}_{(t)} = \bar{\mathbf{M}}\left[\ddot{\boldsymbol{\theta}}_{\mathbf{d}(t)} + \mathbf{K_D}\left(\dot{\boldsymbol{\theta}}_{\mathbf{d}(t)} - \dot{\boldsymbol{\theta}}_{(t)}\right) + \mathbf{K_P}\left(\boldsymbol{\theta}_{\mathbf{d}(t)} - \boldsymbol{\theta}_{(t)}\right)\right] + \hat{\mathbf{H}}_{(t)} + \Delta\mathbf{H}_{(t-L)} \qquad (2.24)$$

$$\hat{\mathbf{H}}_{(t)} = \boldsymbol{\tau}_{(t-L)} - \bar{\mathbf{M}}\ddot{\boldsymbol{\theta}}_{(t-L)}$$

$$\Delta\mathbf{H}_{(t-L)} = \bar{\mathbf{M}}\left[\left(\ddot{\boldsymbol{\theta}}_{\mathbf{d}(t-L)} - \ddot{\boldsymbol{\theta}}_{(t-L)}\right) + \mathbf{K_D}\left(\dot{\boldsymbol{\theta}}_{\mathbf{d}(t-L)} - \dot{\boldsymbol{\theta}}_{(t-L)}\right) + \mathbf{K_P}\left(\boldsymbol{\theta}_{\mathbf{d}(t-L)} - \boldsymbol{\theta}_{(t-L)}\right)\right] + \Delta\mathbf{H}_{(t-2L)}$$

2.2.4 Analysis

This section shows the frequency response characteristic of ETDC. And characteristic of

ETDC is compared with characteristic of TDC in terms of low and high frequency range. In order to

derive ETDC's error dynamics, the torque in ETDC raw (2.24) is substituted by torque of equation (2.2)

as follows:

$$\bar{\mathbf{M}}\left[\left(\ddot{\boldsymbol{\theta}}_{\mathbf{d}(t)} - \ddot{\boldsymbol{\theta}}_{(t)}\right) + \mathbf{K_D}\left(\dot{\boldsymbol{\theta}}_{\mathbf{d}(t)} - \dot{\boldsymbol{\theta}}_{(t)}\right) + \mathbf{K_P}\left(\boldsymbol{\theta}_{\mathbf{d}(t)} - \boldsymbol{\theta}_{(t)}\right)\right] + \Delta\mathbf{H}_{(t-L)} = \mathbf{H}_{(t)} - \hat{\mathbf{H}}_{(t)} \qquad (2.25)$$

$$\Delta\mathbf{H}_{(t-L)} = \bar{\mathbf{M}}\left[\left(\ddot{\boldsymbol{\theta}}_{\mathbf{d}(t-L)} - \ddot{\boldsymbol{\theta}}_{(t-L)}\right) + \mathbf{K_D}\left(\dot{\boldsymbol{\theta}}_{\mathbf{d}(t-L)} - \dot{\boldsymbol{\theta}}_{(t-L)}\right) + \mathbf{K_P}\left(\boldsymbol{\theta}_{\mathbf{d}(t-L)} - \boldsymbol{\theta}_{(t-L)}\right)\right] + \Delta\mathbf{H}_{(t-2L)}$$

In equation (2.25), TDE error term is substituted by equation (2.23) and right side term of the

equation is described by definition of TDE error (2.11) as follows:

$$\bar{\mathbf{M}}\big[\big(\ddot{\boldsymbol{\theta}}_{\mathbf{d}(t)} - \ddot{\boldsymbol{\theta}}_{(t)}\big) + \mathbf{K_D}\big(\dot{\boldsymbol{\theta}}_{\mathbf{d}(t)} - \dot{\boldsymbol{\theta}}_{(t)}\big) + \mathbf{K_P}\big(\boldsymbol{\theta}_{\mathbf{d}(t)} - \boldsymbol{\theta}_{(t)}\big)\big] \tag{2.26}$$

$$+\bar{\mathbf{M}}\big[\big(\ddot{\boldsymbol{\theta}}_{\mathbf{d}(t-L)} - \ddot{\boldsymbol{\theta}}_{(t-L)}\big) + \mathbf{K_D}\big(\dot{\boldsymbol{\theta}}_{\mathbf{d}(t-L)} - \dot{\boldsymbol{\theta}}_{(t-L)}\big) + \mathbf{K_P}\big(\boldsymbol{\theta}_{\mathbf{d}(t-L)} - \boldsymbol{\theta}_{(t-L)}\big)\big]$$

$$+\bar{\mathbf{M}}\big[\big(\ddot{\boldsymbol{\theta}}_{\mathbf{d}(t-2L)} - \ddot{\boldsymbol{\theta}}_{(t-2L)}\big) + \mathbf{K_D}\big(\dot{\boldsymbol{\theta}}_{\mathbf{d}(t-2L)} - \dot{\boldsymbol{\theta}}_{(t-2L)}\big) + \mathbf{K_P}\big(\boldsymbol{\theta}_{\mathbf{d}(t-2L)} - \boldsymbol{\theta}_{(t-2L)}\big)\big]$$

$$\bullet\bullet\bullet$$

$$+\bar{\mathbf{M}}\big[\big(\ddot{\boldsymbol{\theta}}_{\mathbf{d}(t-kL)} - \ddot{\boldsymbol{\theta}}_{(t-kL)}\big) + \mathbf{K_D}\big(\dot{\boldsymbol{\theta}}_{\mathbf{d}(t-kL)} - \dot{\boldsymbol{\theta}}_{(t-kL)}\big) + \mathbf{K_P}\big(\boldsymbol{\theta}_{\mathbf{d}(t-kL)} - \boldsymbol{\theta}_{(t-kL)}\big)\big] = \Delta\mathbf{H}_{(t)}$$

Laplace transform is applied to error dynamics (2.26) with an assumption that time t is sufficient as

follows:

$$\bar{\mathbf{M}}[s^2\mathbf{E}(s) + \mathbf{K_D}s\mathbf{E}(s) + \mathbf{K_P}\mathbf{E}(s)] \tag{2.27}$$

$$+\bar{\mathbf{M}}[s^2\mathbf{E}(s)e^{-Ls} + \mathbf{K_D}s\mathbf{E}(s)e^{-Ls} + \mathbf{K_P}\mathbf{E}(s)e^{-Ls}]$$

$$+\bar{\mathbf{M}}[s^2\mathbf{E}(s)e^{-2Ls} + \mathbf{K_D}s\mathbf{E}(s)e^{-2Ls} + \mathbf{K_P}\mathbf{E}(s)e^{-2Ls}]$$

$$\bullet\bullet\bullet$$

$$+\bar{\mathbf{M}}[s^2\mathbf{E}(s)e^{-kLs} + \mathbf{K_D}s\mathbf{E}(s)e^{-kLs} + \mathbf{K_P}\mathbf{E}(s)e^{-kLs}] = \Delta\mathbf{H}(s)$$

Where $\mathbf{E}(s)$ is Laplace transform of $\boldsymbol{\theta}_{\mathbf{d}(t)} - \boldsymbol{\theta}_{(t)}$: $\mathbf{e}_{(t)} \overset{\mathcal{L}}{\rightarrow} \mathbf{E}(s)$. And e^{-Ls} is time delay of L in Laplace

transform.

Rearranging equation (2.27) as follows:

$$\overline{\mathbf{M}}[(\mathbf{I}s^2 + \mathbf{K_D}s + \mathbf{K_P}) + (\mathbf{I}s^2 + \mathbf{K_D}s + \mathbf{K_P})(e^{-Ls} + e^{-2Ls} + \cdots + e^{-kLs})]\mathbf{E}(s) = \Delta\mathbf{H}(s) \qquad (2.28)$$

Where $\mathbf{I}$ is the identity matrix.

Equation (2.28) can be rearranged by using the sum of geometric sequence as follows:

$$\overline{\mathbf{M}}\left[(\mathbf{I}s^2 + \mathbf{K_D}s + \mathbf{K_P}) + (\mathbf{I}s^2 + \mathbf{K_D}s + \mathbf{K_P})\left(e^{-Ls}\frac{1-e^{-Lsk}}{1-e^{-Ls}}\right)\right]\mathbf{E}(s) = \Delta\mathbf{H}(s) \qquad (2.29)$$

In geometric sequence, first term is e^{-Ls} and common ratio is e^{-Ls}.

Rearranging equation (2.29) as follows:

$$\overline{\mathbf{M}}\left[(\mathbf{I}s^2 + \mathbf{K_D}s + \mathbf{K_P})\left(\frac{1-e^{-Ls(k+1)}}{1-e^{-Ls}}\right)\right]\mathbf{E}(s) = \Delta\mathbf{H}(s) \qquad (2.30)$$

If each joint is individually analyzed, equation (2.30) can be described regarding arbitrary joint i as

follows:

$$\overline{M}_{ii}(s^2 + K_{Dii}s + K_{Pii})\left(\frac{1-e^{-Ls(k+1)}}{1-e^{-Ls}}\right)E_i(s) = \Delta H_i(s) \qquad (2.31)$$

Where $\overline{M}_{ii}$: ith diagonal element of $\overline{\mathbf{M}}$, K_{Dii}: ith diagonal element of $\mathbf{K_D}$, K_{Pii}: ith diagonal element

of $\mathbf{K_P}$, $E_i(s)$: ith element of $\mathbf{E}(s)$, and $\Delta H_i(s)$: ith element of $\Delta\mathbf{H}(s)$.

Transfer function is described from equation (2.31) as follows:

$$\frac{E_i(s)}{\Delta H_i(s)} = \frac{\bar{M}_{ii}^{-1}}{(s^2 + K_{Dii}s + K_{Pii})} \left(\frac{1 - e^{-Ls}}{1 - e^{-Ls(k+1)}} \right) \tag{2.32}$$

In order to analyze frequency response characteristic of ETDC and TDC, transfer functions of ETDC

described in equation (2.32) and transfer function of TDC [Appendix A] are used. Bode magnitude plot

and parameters are shown as follows:

From figure 2.2, ETDC shows that robustness in terms of error is better than TDC in low frequency

range when TDE error is given as input However, in high frequency range, ETDC's error rapidly

fluctuates and looks to be in an unstable state. Then, ETDC and TDC are applied to real robot system

to analyze characteristic of error. Consequently, overall range of the tracking error is reduced.

However, ETDC shows chattering problems in real system. The experimentation regarding ETDC is

shown in appendix B.
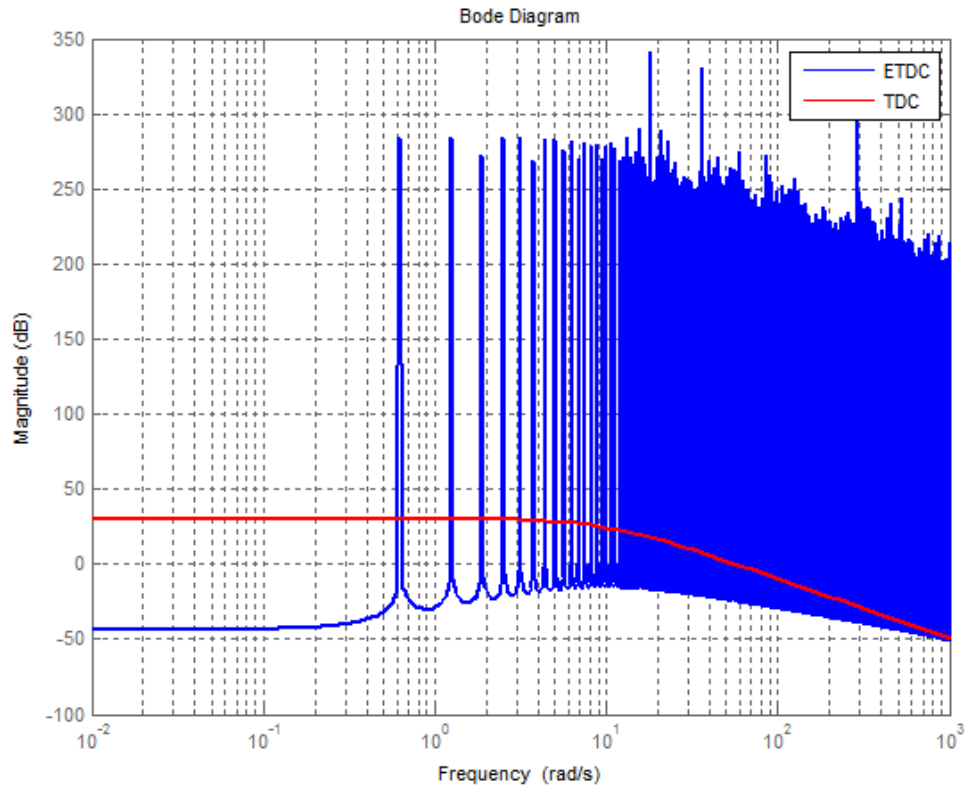
Fig. 2.2 Bode magnitude plots of TDC and ETDC

Controller	$\bar{M}_{ii}$	K_{Dii}	K_{Pii}	L	k
TDC	0.0003	20	100	0.002	-
ETDC	0.0003	20	100	0.002	5000

Table 2.1 Parameters of TDC and ETDC

III . Design and Analysis of Proposed Control

3.1 Outline

Enhanced Time Delay Control (ETDC) shows better performance than Time Delay Control

(TDC) because ETDC complements Time Delay Estimation (TDE) error of TDC. Comparing the

advantages of TDC and ETDC, TDC is more robust in terms of noise like chattering problems, while

ETDC generally shows better performance in terms of tracking errors than TDC. The proposed control

is robust in terms of the noise and shows similar control performances like ETDC.

In chapter 3.2, design method of the new control is introduced and, in chapter 3.3, the proposed

control is compared with ETDC and TDC in frequency response characteristics. Chapter 3.4

describes the discussion regarding the proposed control.

3.2 Design of proposed control

New control scheme proposes to alleviate the noise including chattering problems in ETDC.

The difference between ETDC and TDC is the TDE error term. This term complements TDE error of

TDC. Consequently, ETDC shows better performance in terms of the range of error than TDC.

However, chattering problems occur in ETDC. If TDE error term in ETDC is removed, ETDC is

equivalent to TDC. Control performance of the ETDC is also equivalent to TDC. The proposed control

contains the TDE error term derived in equation (2.22) to keep the control performance of ETDC. And,

the TDE error term is combined with a certain gain to control the TDE error term. The gain is

designates as $\mathbf{K_C}$ and called characteristic gain. The proposed control consists of ETDC derived in

equation (2.24) and the gain as follows:

$$\boldsymbol{\tau}_{(t)} = \overline{\mathbf{M}}\big[\ddot{\boldsymbol{\theta}}_{\mathbf{d}(t)} + \mathbf{K_D}\big(\dot{\boldsymbol{\theta}}_{\mathbf{d}(t)} - \dot{\boldsymbol{\theta}}_{(t)}\big) + \mathbf{K_P}\big(\boldsymbol{\theta}_{\mathbf{d}(t)} - \boldsymbol{\theta}_{(t)}\big)\big] + \widehat{\mathbf{H}}_{(t)} + \mathbf{K_C}\Delta\mathbf{H}_{(t-L)} \tag{3.1}$$

$$\widehat{\mathbf{H}}_{(t)} = \boldsymbol{\tau}_{(t-L)} - \overline{\mathbf{M}}\ddot{\boldsymbol{\theta}}_{(t-L)}$$

$$\Delta\mathbf{H}_{(t-L)} = \overline{\mathbf{M}}\big[\big(\ddot{\boldsymbol{\theta}}_{\mathbf{d}(t-L)} - \ddot{\boldsymbol{\theta}}_{(t-L)}\big) + \mathbf{K_D}\big(\dot{\boldsymbol{\theta}}_{\mathbf{d}(t-L)} - \dot{\boldsymbol{\theta}}_{(t-L)}\big) + \mathbf{K_P}\big(\boldsymbol{\theta}_{\mathbf{d}(t-L)} - \boldsymbol{\theta}_{(t-L)}\big)\big] + \Delta\mathbf{H}_{(t-2L)}$$

Where $\bar{\mathbf{M}}$ is diagonal constant matrix and $\hat{\mathbf{H}}$ is estimation value of $\mathbf{H}$. $\mathbf{K_D}$, $\mathbf{K_P}$ and $\mathbf{K_C}$ are $n \times n$

diagonal matrix of proportional gain, $n \times n$ diagonal matrix of differential gain, and $n \times n$ diagonal

matrix of characteristic gain respectively.

Range of the gain is limited as follows:

$$0 < \mathbf{K_C} < 1 \qquad (3.2)$$

When the gain $\mathbf{K_C}$ is close to 1, the proposed controller behavior is close to ETDC. However, when

the gain $\mathbf{K_C}$ is close to 0, the proposed controller behavior is close to TDC. In the proposed control

scheme, characteristic of the controller is decided by the characteristic gain due to above reasons.

And, in the proposed controller, the TDE error term includes the previous TDE error term. Hence the

new controller is named as an Enhanced Time-Delay Control using a Second-Order Time-Delay

Estimation. The new controller will be concisely called as NEW

3.3 Analysis of the Proposed Control

Chapter 3.2 described the design method of An Enhanced Time-Delay Control using a

Second-Order Time-Delay Estimation (NEW). This chapter shows the analysis of NEW in terms of

frequency response characteristic and NEW is compared with ETDC and TDC in the analysis. To

derive error dynamics of NEW, torque in NEW is substituted by torque of the general dynamics of

robot manipulators described in equation (2.1) as follows:

$$\bar{\mathbf{M}}[\ddot{\mathbf{e}}_{(t)} + \mathbf{K_D}\dot{\mathbf{e}}_{(t)} + \mathbf{K_P}\mathbf{e}_{(t)}] + \mathbf{K_C}\Delta\mathbf{H}_{(t-L)} = \Delta\mathbf{H}_{(t)} \qquad (3.3)$$

$$\Delta\mathbf{H}_{(t-L)} = \bar{\mathbf{M}}[(\ddot{\boldsymbol{\theta}}_{\mathbf{d}(t-L)} - \ddot{\boldsymbol{\theta}}_{(t-L)}) + \mathbf{K_D}(\dot{\boldsymbol{\theta}}_{\mathbf{d}(t-L)} - \dot{\boldsymbol{\theta}}_{(t-L)}) + \mathbf{K_P}(\boldsymbol{\theta}_{\mathbf{d}(t-L)} - \boldsymbol{\theta}_{(t-L)})] + \Delta\mathbf{H}_{(t-2L)}$$

Rearranging equation (3.3) with the TDE error term described in equation (2.23), the error dynamics

can be described as follows:

$$\bar{\mathbf{M}}[\ddot{\mathbf{e}}_{(t)} + \mathbf{K_D}\dot{\mathbf{e}}_{(t)} + \mathbf{K_P}\mathbf{e}_{(t)}] \qquad (3.4)$$

$$+\mathbf{K_C}\bar{\mathbf{M}}[(\ddot{\boldsymbol{\theta}}_{\mathbf{d}(t-L)} - \ddot{\boldsymbol{\theta}}_{(t-L)}) + \mathbf{K_D}(\dot{\boldsymbol{\theta}}_{\mathbf{d}(t-L)} - \dot{\boldsymbol{\theta}}_{(t-L)}) + \mathbf{K_P}(\boldsymbol{\theta}_{\mathbf{d}(t-L)} - \boldsymbol{\theta}_{(t-L)})$$

$$+(\ddot{\boldsymbol{\theta}}_{\mathbf{d}(t-2L)} - \ddot{\boldsymbol{\theta}}_{(t-2L)}) + \mathbf{K_D}(\dot{\boldsymbol{\theta}}_{\mathbf{d}(t-2L)} - \dot{\boldsymbol{\theta}}_{(t-2L)}) + \mathbf{K_P}(\boldsymbol{\theta}_{\mathbf{d}(t-2L)} - \boldsymbol{\theta}_{(t-2L)})$$

$$\bullet\bullet\bullet$$

$$+(\ddot{\boldsymbol{\theta}}_{\mathbf{d}(t-kL)} - \ddot{\boldsymbol{\theta}}_{(t-kL)}) + \mathbf{K_D}(\dot{\boldsymbol{\theta}}_{\mathbf{d}(t-kL)} - \dot{\boldsymbol{\theta}}_{(t-kL)}) + \mathbf{K_P}(\boldsymbol{\theta}_{\mathbf{d}(t-kL)} - \boldsymbol{\theta}_{(t-kL)})] = \Delta\mathbf{H}_{(t)}$$

Where k is the operation count.

Laplace transform is applied to error dynamics (3.4) with an assumption that time t is sufficiently large as follows:

$$\bar{\mathbf{M}}[s^2\mathbf{E}(s) + \mathbf{K_D}s\mathbf{E}(s) + \mathbf{K_P}\mathbf{E}(s)] \tag{3.5}$$

$$+\mathbf{K_C}\bar{\mathbf{M}}[s^2\mathbf{E}(s)e^{-Ls} + \mathbf{K_D}s\mathbf{E}(s)e^{-Ls} + \mathbf{K_P}\mathbf{E}(s)e^{-Ls}$$

$$+s^2\mathbf{E}(s)e^{-2Ls} + \mathbf{K_D}s\mathbf{E}(s)e^{-2Ls} + \mathbf{K_P}\mathbf{E}(s)e^{-2Ls}$$

$$\bullet\bullet\bullet$$

$$+s^2\mathbf{E}(s)e^{-kLs} + \mathbf{K_D}s\mathbf{E}(s)e^{-kLs} + \mathbf{K_P}\mathbf{E}(s)e^{-kLs}] = \Delta\mathbf{H}(s)$$

Where $\mathbf{E}(s)$ is Laplace transform of $\boldsymbol{\theta}_{\mathbf{d}(t)} - \boldsymbol{\theta}_{(t)}$: $\mathbf{e}_{(t)}\xrightarrow{\mathcal{L}}\mathbf{E}(s)$. And e^{-Ls} is time delay of L in Laplace transform.

Rearranging equation (3.5) as follows:

$$\bar{\mathbf{M}}(\mathbf{I}s^2 + \mathbf{K_D}s + \mathbf{K_P})\mathbf{E}(s) \tag{3.6}$$

$$+\mathbf{K_C}\bar{\mathbf{M}}[(\mathbf{I}s^2 + \mathbf{K_D}s + \mathbf{K_P})(e^{-Ls} + e^{-2Ls} +\bullet\bullet\bullet +e^{-kLs})]\mathbf{E}(s) = \Delta\mathbf{H}(s)$$

Where $\mathbf{I}$ is the identity matrix.

Equation (3.6) can be rearranged by using sum of geometric sequence as follows:

$$\bar{\mathbf{M}}(\mathbf{I}s^2 + \mathbf{K_D}s + \mathbf{K_P})\mathbf{E}(s)$$

$$+\mathbf{K_C}\bar{\mathbf{M}}[(\mathbf{I}s^2 + \mathbf{K_D}s + \mathbf{K_P})\left(e^{-Ls}\frac{1-e^{-Lsk}}{1-e^{-Ls}}\right)]\mathbf{E}(s) = \Delta\mathbf{H}(s) \tag{3.7}$$

In geometric sequence, first term is e^{-Ls} and common ratio is e^{-Ls}.

If each joint is individually analyzed, equation (3.7) can be described regarding arbitrary joint i as follows:

$$\bar{M}_{ii}(s^2 + K_{Dii}s + K_{Pii})E_i(s) \tag{3.8}$$

$$+K_{Cii}\bar{M}_{ii}(s^2 + K_{Dii}s + K_{Pii})\left(\frac{1-e^{-Ls(k+1)}}{1-e^{-Ls}}\right)E_i(s) = \Delta H_i(s)$$

Where $\bar{M}_{ii}$: ith diagonal element of $\bar{\mathbf{M}}$, K_{Dii}: ith diagonal element of $\mathbf{K_D}$, K_{Pii}: ith diagonal element of $\mathbf{K_P}$, K_{Cii}: ith diagonal element of $\mathbf{K_C}$, $E_i(s)$: ith element of $\mathbf{E}(s)$, and $\Delta H_i(s)$: $i th$ element of $\Delta\mathbf{H}(s)$.

Rearranging equation (3.8) as follows:

$$\bar{M}_{ii}(s^2 + K_{Dii}s + K_{Pii})E_i(s)\left(\frac{1+(K_{Cii}-1)e^{-Ls}-K_{Cii}e^{-Ls(k+1)}}{1-e^{-Ls}}\right) = \Delta H_i(s) \tag{3.9}$$

Transfer function of NEW is described from equation (3.9) as follows:

$$\frac{E_i(s)}{\Delta H_i(s)} = \frac{\bar{M}_{ii}^{-1}}{(s^2 + K_{Dii}s + K_{Pii})} \left(\frac{1 - e^{-Ls}}{1 + (K_{Cii} - 1)e^{-Ls} - K_{Cii}e^{-Ls(k+1)}} \right) \tag{3.10}$$

To analyze frequency response characteristic of NEW, the transfer function of NEW is shown and the

transfer function is compared with transfer function of ETDC and TDC as follows:

Parameters of NEW, ETDC, and TDC are displayed as follows:

In the results of frequency response characteristic, input values are TDE error and output values are

the error; it is the difference between desired position and measured position from the sensors. In low

frequency range, NEW's errors are mostly lower under TDC's errors. It means that NEW is more

robust than TDC in terms of low frequency TDE error. In high frequency range, magnitude of errors

like the spike in NEW is less than ETDC in terms of high frequency TDE error. In other words, when

high frequency TDE errors are inputted to NEW and ETDC, NEW is more robust than ETDC in terms
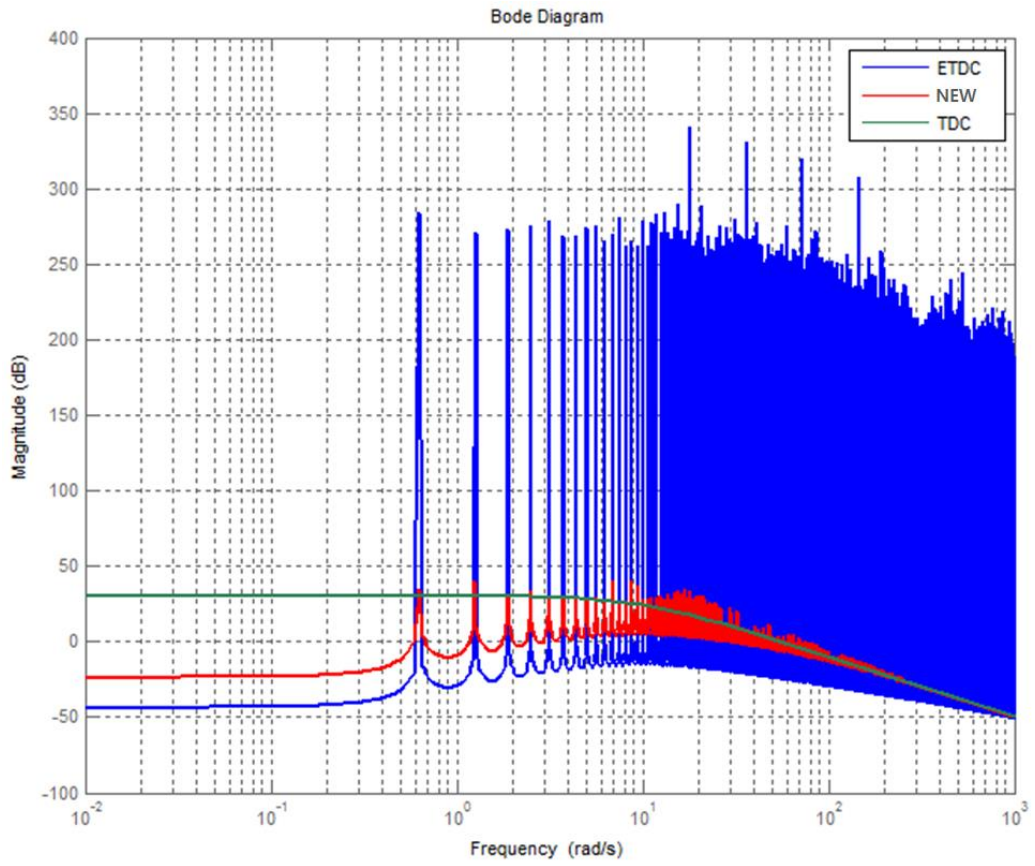
of the TDE error as the input.

Fig. 3.1 Bode magnitude plots of NEW, ETDC, and TDC

Controller	$\bar{M}_{ii}$	K_{Dii}	K_{Pii}	K_{Cii}	L	k
TDC	0.0003	20	100	-	0.002	-
ETDC	0.0003	20	100	-	0.002	5000
NEW	0.0003	20	100	0.1	0.002	5000

Table 3.1 Parameters of NEW, ETDC, and TDC

3.4 Discussion

NEW is proposed to alleviate the noise in ETDC. The proposed controller is derived from

ETDC and the characteristic gain. It is easily implemented like the ETDC. Characteristic of NEW is

decided by tuning the characteristic gain in NEW. When the gain is close to zero, NEW shows TDC's

characteristic of control and stability. And, when the gain is close to one, NEW shows ETDC's

characteristic of control and stability. In the frequency response characteristic, the characteristic gain

in NEW is tuned as 0.1. Consequently, NEW shows that robustness in terms of TDE error is less than

ETDC in low frequency range. However, robustness of NEW is better than ETDC in high frequency

range. The gain $\bar{\mathbf{M}}$ of NEW is same with the gain $\bar{\mathbf{M}}$ of ETDC in frequency response characteristic

analysis. However, in real system, the gains of both NEW and ETDC are optimally tuned as

appropriate values to derive best performance. Consequently, experimentation regarding NEW and

ETDC with the same gains will be shown to confirm the results of frequency response characteristics.

Also, when the characteristic gain of NEW is changed, control performance of NEW will be shown to

check the effect of the gain in NEW. And then, experimentation regarding NEW and ETDC with best

tuned gains will be shown to introduce advantages of NEW.

IV . Simulation

In this chapter, NEW on robot manipulator is simulated to check possibility of its

implementation. And NEW is compared with ETDC in terms of control performance. The plant

includes Coulomb friction, viscous friction, and gravity term. In addition, both controllers show control

performance in an environment with two links robot manipulator on simulation to prove usefulness in

multi-joint robots.

4.1 One Link Robot Manipulator

4.1.1 Plant for the one link manipulator simulation

The controllers are simulated on a plant with one link robot manipulator. The plant is shown

in figure 4.1. m, l, and g are mass of the link, length of link, and acceleration of gravity respectively.

Here, mass is assumed as concentrated mass at the end of the link, and friction is influenced on the

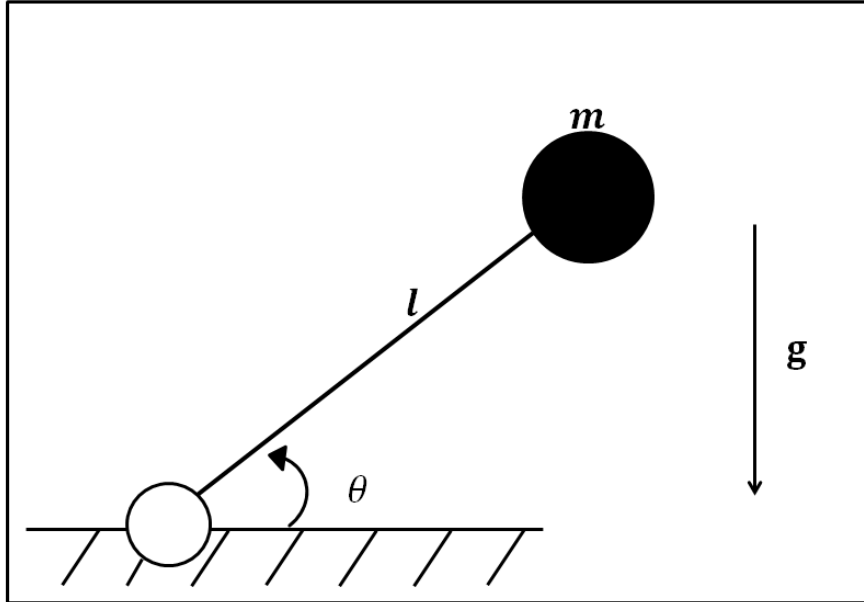joint. Also, gravity exerts vertical influence.

Fig. 4.1 One link robot manipulator

Dynamics of robot manipulator is represented as follows:

$$M(\theta)\ddot{\theta} + V(\theta,\dot{\theta}) + G(\theta) + F(\theta,\dot{\theta}) = \tau \tag{4.1}$$

Where $M = ml^2$, $V = 0$, $G = mgl\cos\theta$, $F = f_c sgn(\dot{\theta}) + f_v\dot{\theta}$

Here, f_c is Coulomb friction coefficient: $f_c = 50\ [Nm]$. f_v is viscous friction coefficient: $f_v =$

5 [Nmsec]. $m = 1.0$ [kg]. $l = 1.0$ [m]. $g = 9.8\ [m/s^2\ ]$

4.1.2 Design of the controllers

ETDC is designed for simulation as follows:

$$\tau_{(t)} = \tau_{(t-L)} - \bar{M}\ddot{\theta}_{(t-L)} + \bar{M}\left[\ddot{\theta}_d + K_D(\dot{\theta}_d - \dot{\theta}) + K_P(\theta_d - \theta)\right] + \Delta H_{(t-L)} \qquad (4.2)$$

$$\Delta H_{(t-L)} = \bar{M}\left[\left(\ddot{\theta}_{d(t-L)} - \ddot{\theta}_{(t-L)}\right) + K_D\left(\dot{\theta}_{d(t-L)} - \dot{\theta}_{(t-L)}\right) + K_P\left(\theta_{d(t-L)} - \theta_{(t-L)}\right)\right] + \Delta H_{(t-2L)}$$

Parameters, $\bar{M}$, K_D, and K_P are set to 0.01, 20, and 100 respectively. In PD gain, natural frequency

is $10\,[\mathrm{rad/sec}]$ and critical damping is used. Also, time of sampling interval and time delay *L* are set

as 0.001 [sec] respectively.

NEW is designed as follows:

$$\tau_{(t)} = \tau_{(t-L)} - \bar{M}\ddot{\theta}_{(t-L)} + \bar{M}\left[\ddot{\theta}_d + K_D(\dot{\theta}_d - \dot{\theta}) + K_P(\theta_d - \theta)\right] + K_C\Delta H_{(t-L)} \qquad (4.3)$$

$$\Delta H_{(t-L)} = \bar{M}\left[\left(\ddot{\theta}_{d(t-L)} - \ddot{\theta}_{(t-L)}\right) + K_D\left(\dot{\theta}_{d(t-L)} - \dot{\theta}_{(t-L)}\right) + K_P\left(\theta_{d(t-L)} - \theta_{(t-L)}\right)\right] + \Delta H_{(t-2L)}$$

Parameters, $\bar{M}$, K_D, K_P, and K_C are set to 0.095, 20, 100, and 0.1 respectively. In PD gain, natural

frequency is $10\,[\mathrm{rad/sec}]$ and critical damping is used. Also, time of sampling interval and time delay

L are set as 0.001 [sec] respectively.

Desired trajectory is described by using fifth-order polynomial trajectory generation scheme as

follows [2]:

$$\theta_d(t) = a_0 + a_1 t + a_2 t^2 + a_3 t^3 + a_4 t^4 + a_5 t^5 \qquad (4.4)$$

$$a_0 = \theta_0,$$

$$a_1 = \dot{\theta}_0,$$

$$a_2 = \frac{\ddot{\theta}_0}{2},$$

$$a_3 = \frac{20\theta_f - 20\theta_0 - (8\dot{\theta}_f + 12\dot{\theta}_0)t_f - (3\ddot{\theta}_0 - \ddot{\theta}_f)t_f^2}{2t_f^3},$$

$$a_4 = \frac{30\theta_0 - 30\theta_f + (14\dot{\theta}_f + 16\dot{\theta}_0)t_f + (3\ddot{\theta}_0 - 2\ddot{\theta}_f)t_f^2}{2t_f^4},$$

$$a_5 = \frac{12\theta_f - 12\theta_0 - (6\dot{\theta}_f + 6\dot{\theta}_0)t_f - (\ddot{\theta}_0 - \ddot{\theta}_f)t_f^2}{2t_f^5}.$$

Where θ_0 is initial value of theta, θ_f is final value of theta, and t_f is finish time.

Values for each of the parameters in equation (4.4) are shown in table (4.1).

Desired input from equation (4.4) and table (4.1) is shown in figure 4.2. In the figure, (a) desired

trajectory and (b) desired velocity are described.

Parameters Time [sec]	θ_0 [Degree]	θ_f [Degree]	t_f [sec]
$0 < t \leq 5$	0	30	5
$5 < t \leq 10$	30	0	10
$10 < t \leq 15$	0	-30	15
$15 < t \leq 20$	-30	0	20

Table 4.1 Desired values of trajectory for one link manipulator simulation

4.1.3 Results of the one link manipulator simulation

Results of simulation are represented in figure 4.3 when ETDC is applied to the one link

manipulator. In the figure, (a), (b), and (c) describe tracking error, velocity error, and input torque of

ETDC respectively. Results of simulation are represented in figure 4.4 when NEW is applied to the

one link manipulator. In the figure, (a), (b), and (c) describe tracking error, velocity error, and input

torque of NEW respectively. In the tracking error graph, errors like spike of ETDC and NEW occur in

about 0, 5, 10, and 15 [sec]. After the spikes of ETDC, tracking errors like noise fluctuate rapidly while

tracking errors of NEW show relatively stable state. The noise like chattering problems of ETDC is

also shown in the velocity error and the torque graph. Control performance of ETDC is degraded by

the phenomena. Hence, ETDC is not suitable when precise control performance is required for robot
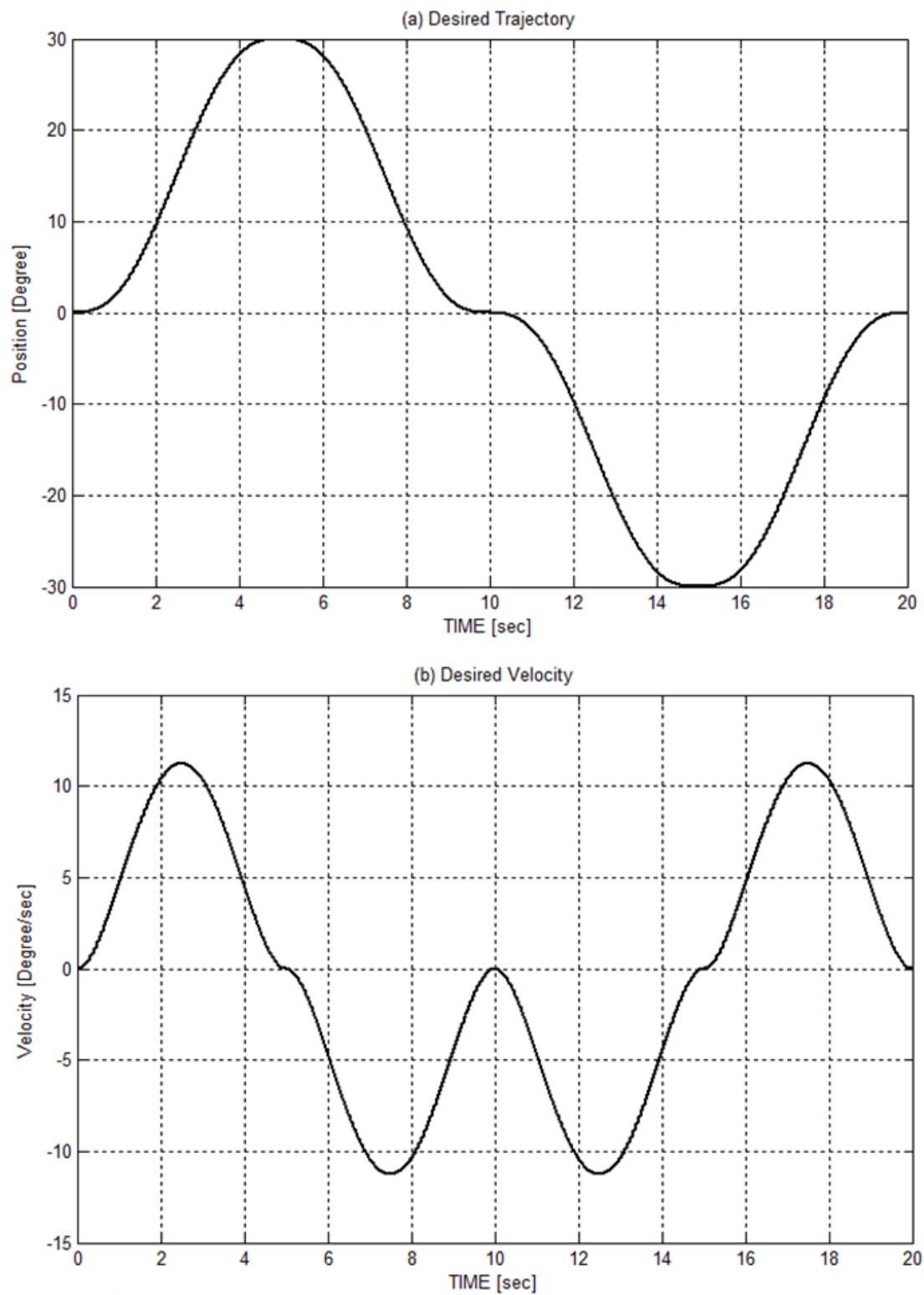
manipulators.

Fig. 4.2 Desired input for one link manipulator simulation:

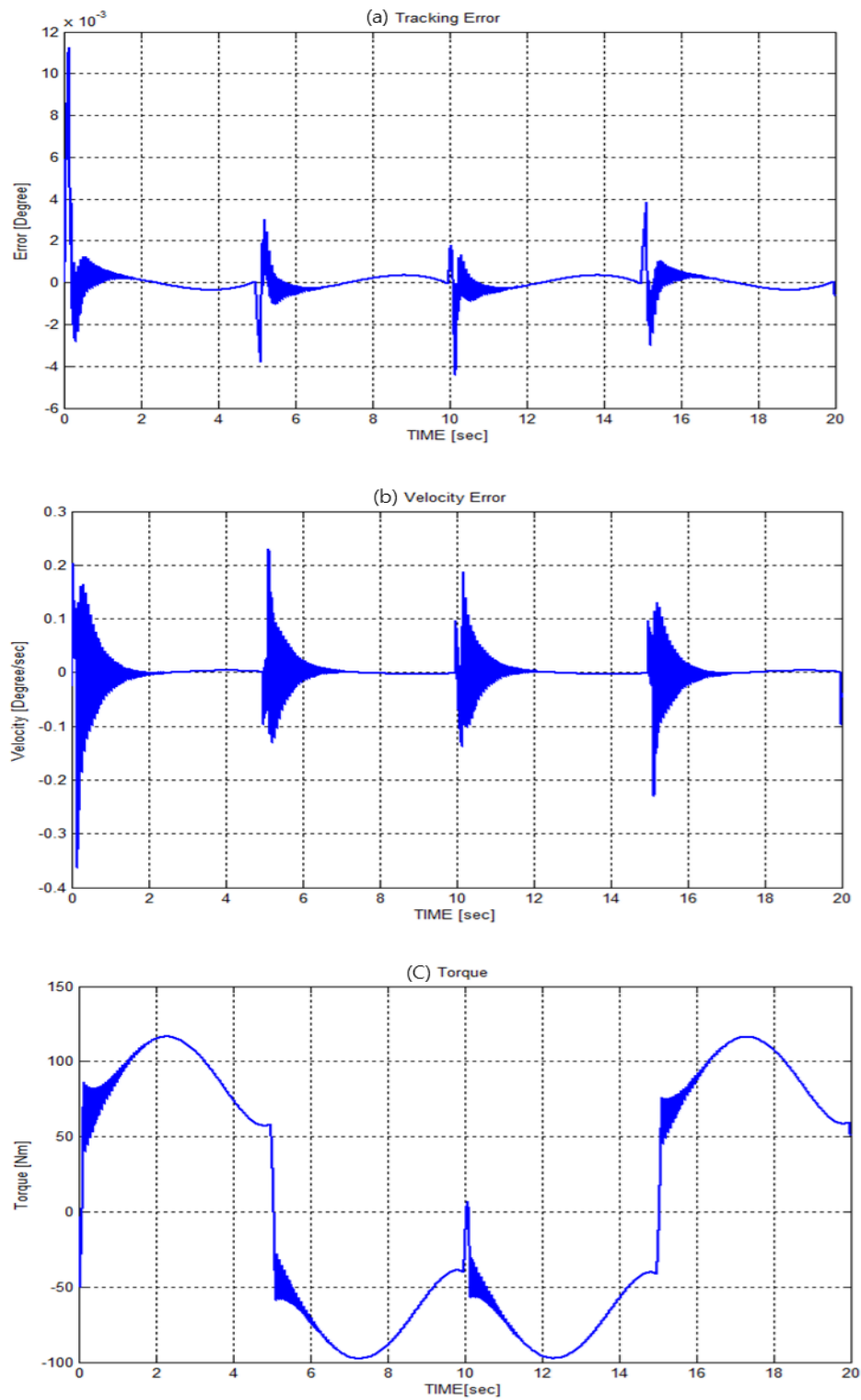(a) desired trajectory (b) desired velocity

Fig. 4.3 Simulation results of ETDC for one link manipulator:

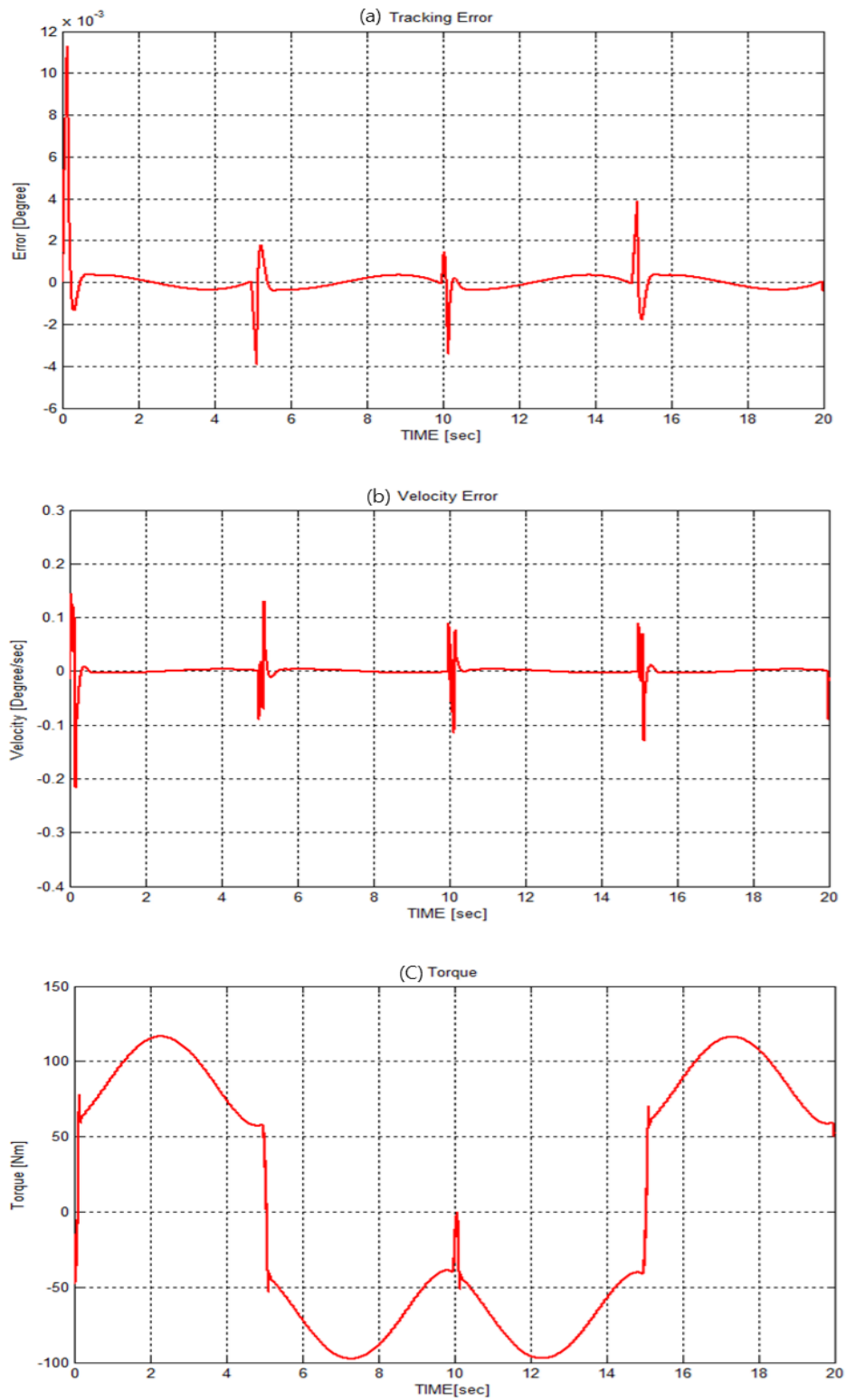(a) Tracking error (b) velocity error (c) torque

Fig. 4.4 Simulation results of NEW for one link manipulator:

(a) tracking error (b) velocity error (c) torque

4.2 Two Links Robot Manipulator

NEW is applied to verify utility in multi joint manipulators. Here, two links robot manipulator is

used and described in figure 4.5. And ETDC and NEW are compared in terms of control performance.

4.2.1 Plant for the two links manipulator simulation

In this simulation, the plant includes Coulomb friction, viscous friction, Coriolis, centrifugal

effect, and gravity effect.

In figure 4.5, m_1, m_2, l_1, l_2, and g are mass of the link 1, link 2, length of link 1, link2, and

acceleration of gravity respectively. Here, mass is assumed as concentrated mass at the end of each

link, and friction is influenced on each joint. Also, gravity is influenced in vertical directions.

Dynamics of robot manipulator is represented as follows:

$$\mathbf{M}(\boldsymbol{\theta})\ddot{\boldsymbol{\theta}} + \mathbf{V}(\boldsymbol{\theta}, \dot{\boldsymbol{\theta}}) + \mathbf{G}(\boldsymbol{\theta}) + \mathbf{F}(\boldsymbol{\theta}, \dot{\boldsymbol{\theta}}) = \boldsymbol{\tau} \qquad (4.5)$$

Where,

$$\mathbf{M} = \begin{bmatrix} (m_1 + m_2)l_1^2 + m_2l_2^2 + 2m_2l_1l_2cos\theta_2 & m_2l_2^2 + m_2l_1l_2cos\theta_2 \\ m_2l_2^2 + m_2l_1l_2cos\theta_2 & m_2l_2^2 \end{bmatrix}$$

- 40 -

$$\mathbf{V} = \begin{bmatrix} -2\dot{\theta}_1\dot{\theta}_2 m_2 l_1 l_2 sin\theta_2 - \dot{\theta}_2^2 m_2 l_1 l_2 sin\theta_2 \\ \dot{\theta}_1^2 m_2 l_1 l_2 sin\theta_2 \end{bmatrix}$$

$$\mathbf{G} = \begin{bmatrix} (m_1 + m_2)gl_1 cos\theta_1 + m_2 gl_2 cos(\theta_1 + \theta_2) \\ m_2 gl_2 cos(\theta_1 + \theta_2) \end{bmatrix}$$

$$\mathbf{F} = \begin{bmatrix} f_{v1}\dot{\theta}_1 + f_{c1} sgn(\dot{\theta}_1) \\ f_{v2}\dot{\theta}_2 + f_{c2} sgn(\dot{\theta}_2) \end{bmatrix}$$

Here, f_c is Coulomb friction coefficient: $f_{c1} = f_{c2} = 1 \ [Nm]$. f_v is viscous friction coefficient:

$f_{v1} = f_{v2} = 1 \ [Nmsec]$. $m_1 = m_2 = 1.0 \ [kg]$. $l_1 = l_2 = 1.0 \ [m]$. $g = 9.81 \ [m/s^2 \ ]$
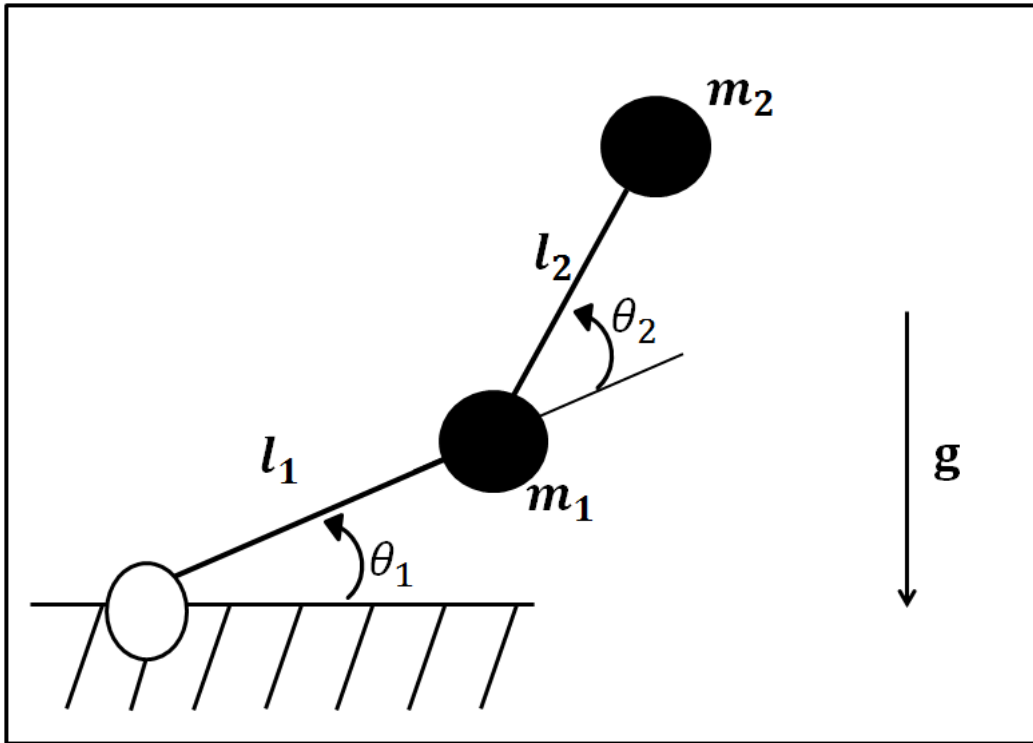

Fig. 4.5 Two links robot manipulator

4.2.2 Design of the controllers

ETDC for this simulation is designed as follows:

$$\boldsymbol{\tau}_{(t)} = \boldsymbol{\tau}_{(t-L)} - \bar{\mathbf{M}}\ddot{\boldsymbol{\theta}}_{(t-L)} + \bar{\mathbf{M}}\big[\ddot{\boldsymbol{\theta}}_{\mathbf{d}(t)} + \mathbf{K_D}\big(\dot{\boldsymbol{\theta}}_{\mathbf{d}(t)} - \dot{\boldsymbol{\theta}}_{(t)}\big) + \mathbf{K_P}\big(\boldsymbol{\theta}_{\mathbf{d}(t)} - \boldsymbol{\theta}_{(t)}\big)\big] + \Delta\mathbf{H}_{(t-L)} \tag{4.6}$$

$$\Delta\mathbf{H}_{(t-L)} = \bar{\mathbf{M}}\big[\big(\ddot{\boldsymbol{\theta}}_{\mathbf{d}(t-L)} - \ddot{\boldsymbol{\theta}}_{(t-L)}\big) + \mathbf{K_D}\big(\dot{\boldsymbol{\theta}}_{\mathbf{d}(t-L)} - \dot{\boldsymbol{\theta}}_{(t-L)}\big) + \mathbf{K_P}\big(\boldsymbol{\theta}_{\mathbf{d}(t-L)} - \boldsymbol{\theta}_{(t-L)}\big)\big] + \Delta\mathbf{H}_{(t-2L)}$$

Where $\bar{\mathbf{M}}$ consist of $\bar{M}_{11} = 0.118$ and $\bar{M}_{22} = 0.159$. $\mathbf{K_D}$=20I and $\mathbf{K_P} = 100\mathbf{I}$. It means that natural

frequency is 10[rad/sec] and critical damping is used.

NEW is designed as follows:

$$\boldsymbol{\tau}_{(t)} = \boldsymbol{\tau}_{(t-L)} - \bar{\mathbf{M}}\ddot{\boldsymbol{\theta}}_{(t-L)} + \bar{\mathbf{M}}\big[\ddot{\boldsymbol{\theta}}_{\mathbf{d}(t)} + \mathbf{K_D}\big(\dot{\boldsymbol{\theta}}_{\mathbf{d}(t)} - \dot{\boldsymbol{\theta}}_{(t)}\big) + \mathbf{K_P}\big(\boldsymbol{\theta}_{\mathbf{d}(t)} - \boldsymbol{\theta}_{(t)}\big)\big] + \mathbf{K_C}\Delta\mathbf{H}_{(t-L)} \tag{4.7}$$

$$\Delta\mathbf{H}_{(t-L)} = \bar{\mathbf{M}}\big[\big(\ddot{\boldsymbol{\theta}}_{\mathbf{d}(t-L)} - \ddot{\boldsymbol{\theta}}_{(t-L)}\big) + \mathbf{K_D}\big(\dot{\boldsymbol{\theta}}_{\mathbf{d}(t-L)} - \dot{\boldsymbol{\theta}}_{(t-L)}\big) + \mathbf{K_P}\big(\boldsymbol{\theta}_{\mathbf{d}(t-L)} - \boldsymbol{\theta}_{(t-L)}\big)\big] + \Delta\mathbf{H}_{(t-2L)}$$

Where $\bar{\mathbf{M}}$ consist of $\bar{M}_{11} = 0.359$ and $\bar{M}_{22} = 0.300$. $\mathbf{K_D}$=20I, $\mathbf{K_P} = 100\mathbf{I}$, and $\mathbf{K_C} = 0.1\mathbf{I}$. Natural

frequency is 10[rad/sec] and critical damping is used.

Desired trajectory is described by using fifth-order polynomial trajectory generation scheme [2] as

follows:

$$\theta_{d1}(t) = \theta_{d2}(t) = a_0 + a_1 t + a_2 t^2 + a_3 t^3 + a_4 t^4 + a_5 t^5 \tag{4.8}$$

$$a_0 = \theta_0,$$

$$a_1 = \dot{\theta}_0,$$

$$a_2 = \frac{\ddot{\theta}_0}{2},$$

$$a_3 = \frac{20\theta_f - 20\theta_0 - (8\dot{\theta}_f + 12\dot{\theta}_0)t_f - (3\ddot{\theta}_0 - \ddot{\theta}_f)t_f^2}{2t_f^3},$$

$$a_4 = \frac{30\theta_0 - 30\theta_f + (14\dot{\theta}_f + 16\dot{\theta}_0)t_f + (3\ddot{\theta}_0 - 2\ddot{\theta}_f)t_f^2}{2t_f^4},$$

$$a_5 = \frac{12\theta_f - 12\theta_0 - (6\dot{\theta}_f + 6\dot{\theta}_0)t_f - (\ddot{\theta}_0 - \ddot{\theta}_f)t_f^2}{2t_f^5}.$$

Where θ_0 is initial value of theta, θ_f is final value of theta, and t_f is finish time.

Then, each value of parameters in equation (4.8) is shown in table 4.2.

Parameters Time [sec]	θ_0 [Degree]	θ_f [Degree]	t_f [sec]
$0 < t \leq 2.5$	0	30	2.5
$2.5 < t \leq 5$	30	0	5
$5 < t \leq 7.5$	0	-30	7.5
$7.5 < t \leq 10$	-30	0	10

Table 4.2 Desired values of trajectory for two links manipulator simulation

Desired input from equation (4.8) and table (4.2) is shown in figure 4.6. In the figure, (a) desired

trajectory and (b) desired velocity are described.

4.2.3 Results of the two links manipulator simulation

Results of simulations are represented in figure 4.6 and 4.7. In two figures, (a), (b), and (c)

are tracking error, velocity error, and torque of joint 1 respectively. And (d), (e), and (f) are tracking

error, velocity error, and torque of joint 2 respectively.

Results of ETDC and NEW are shown in figure 4.6 and 4.7 respectively. In the figures, ETDC's

errors like the spike in 2.5 and 7.5 [sec] are less than NEW. However, ETDC's errors in initial part are

shown like chattering problems. Also, initial parts of velocity error and torque of ETDC show that

values of velocity and torque are changed rapidly. Such phenomenon is not suitable when exquisite

control performance is required.

In the two links manipulator on simulation, NEW is verified by the results. Hence, NEW is suitable to application for multi-joint robots. In next chapter, NEW will be applied to six Degrees Of Freedom (DOF) robot: Samsung FARAMAN AT2.
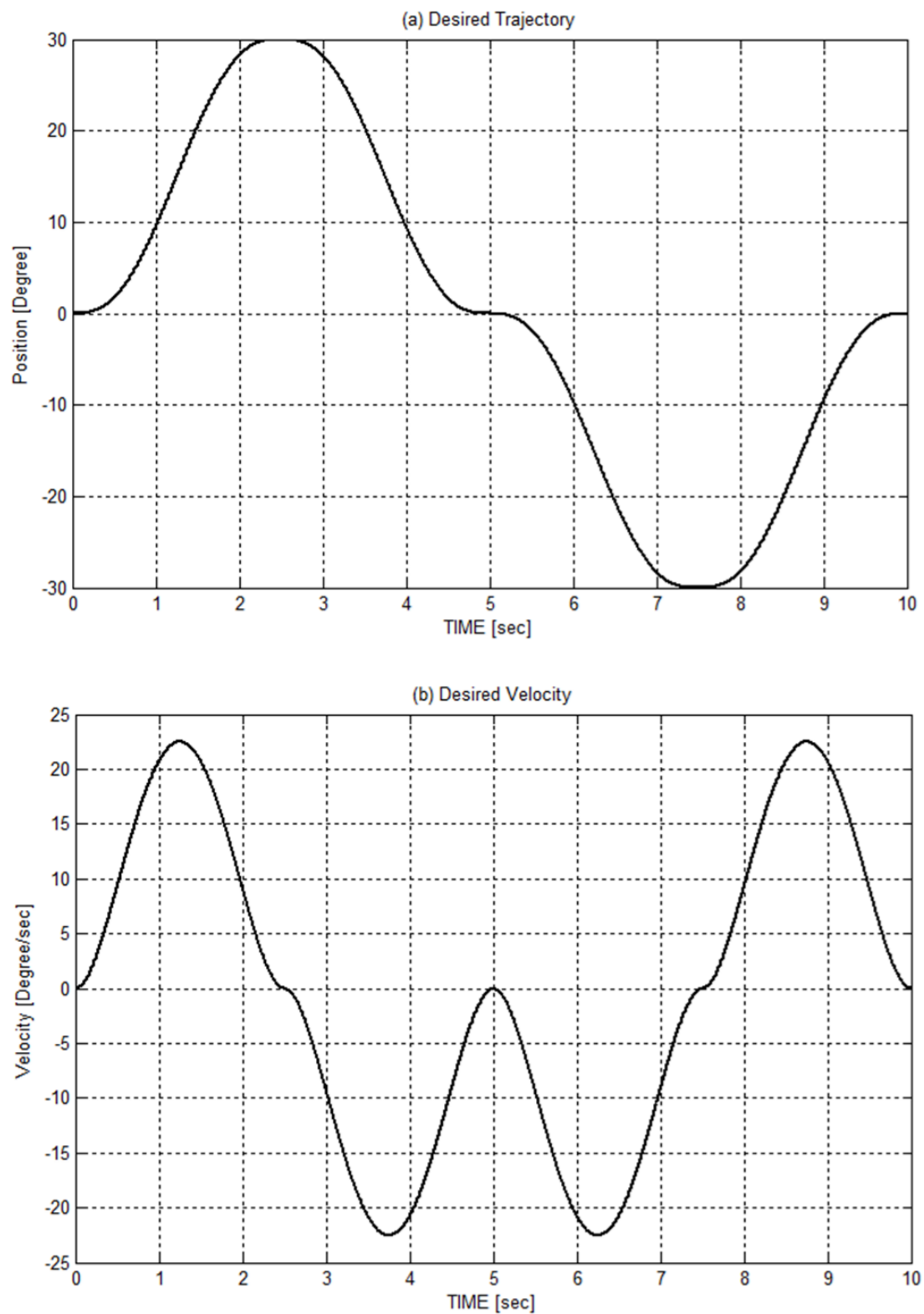
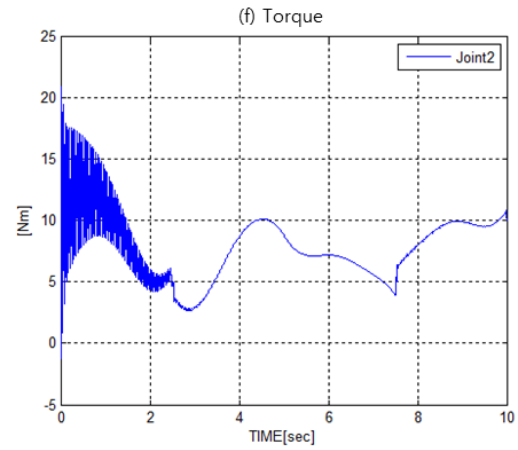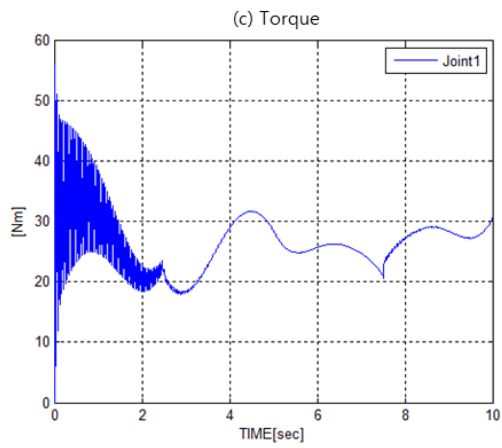Fig. 4.6 Desired input for two links manipulator: (a) desired trajectory (b) desired velocity
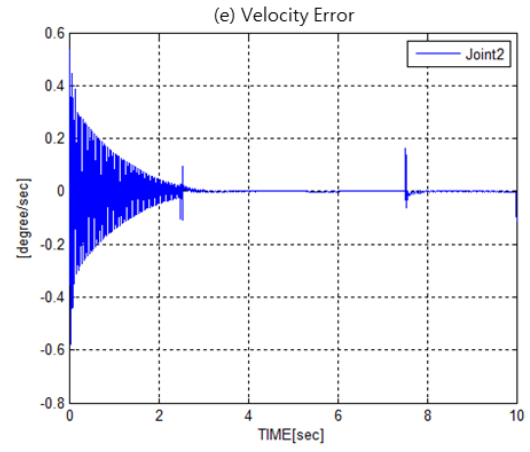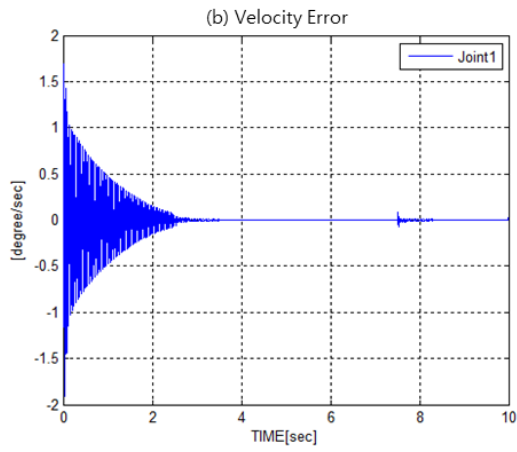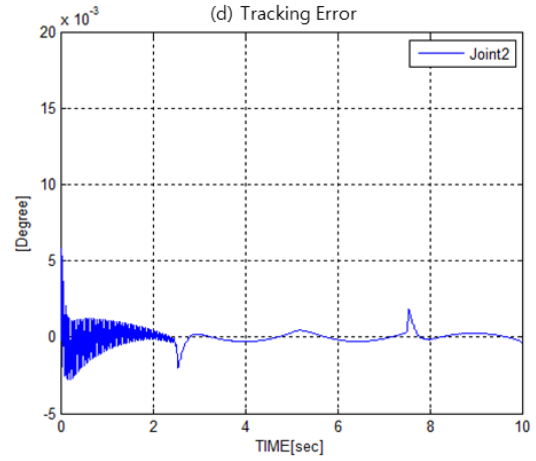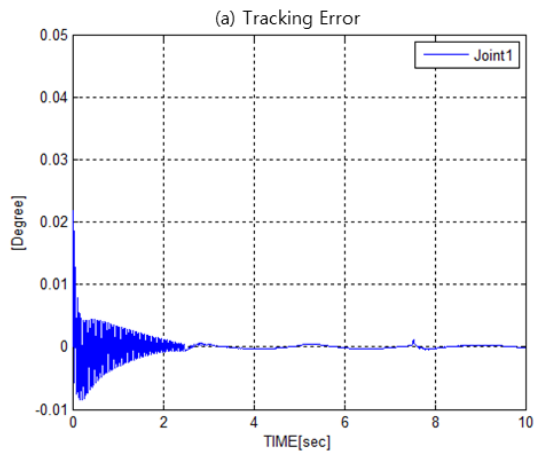
Fig. 4.7 Simulation results of ETDC for two links manipulator:

(a) tracking error at joint 1 (b) velocity error at joint 1 (c) torque at joint 1

(d) tracking error at joint 2 (e) velocity error at joint 2 (f) torque at joint 2

Fig. 4.8 Simulation results of NEW for two links manipulator:

(a) tracking error at joint 1 (b) velocity error at joint 1 (c) torque at joint 1

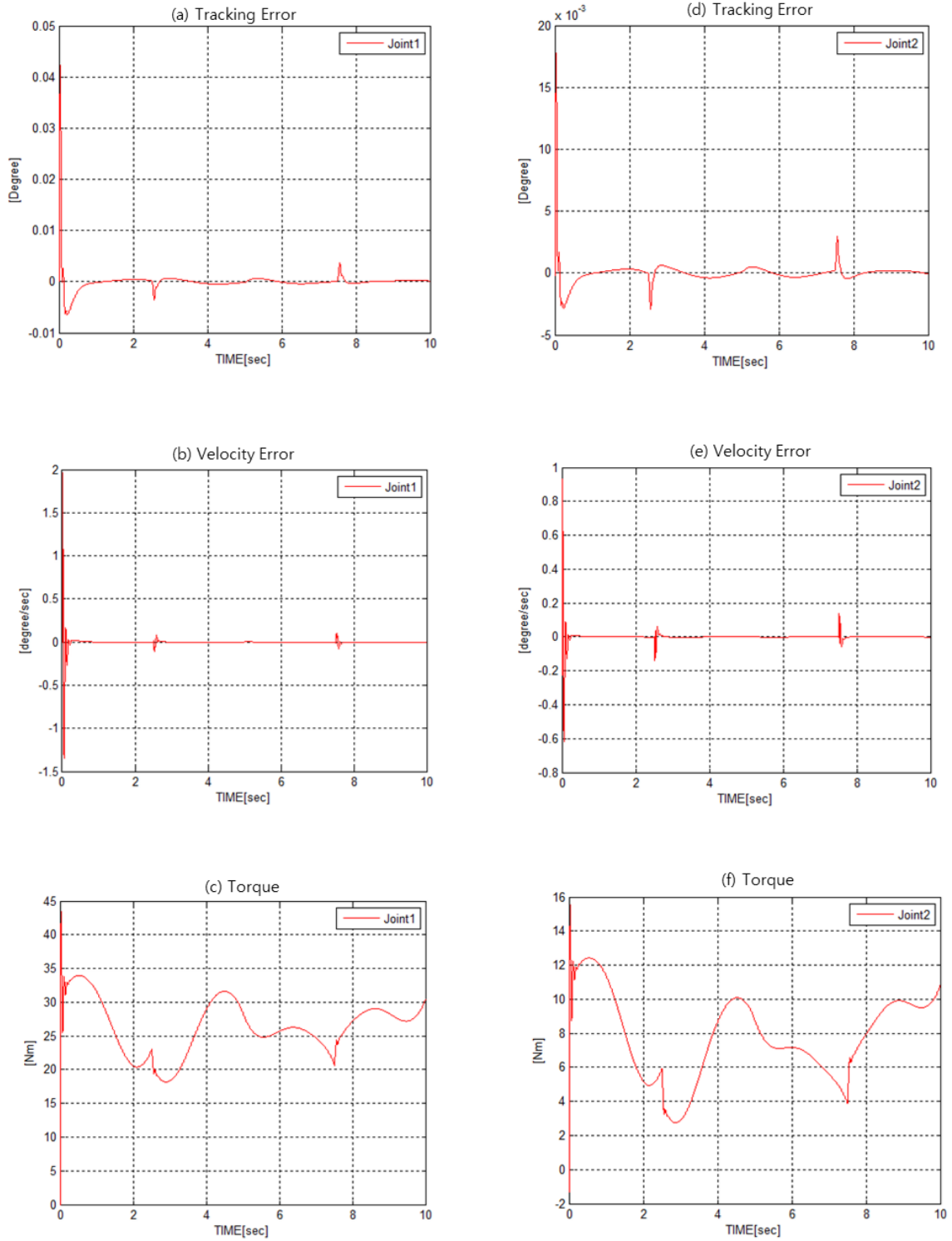(d) tracking error at joint 2 (e) velocity error at joint 2 (f) torque at joint 2

Ⅴ. Experimentations

Six degree of freedom (DOF) robot is used for the experimentations to show control performance. NEW's control performance is compared with ETDC's control performance. In the results, the noise including chattering problems is especially highlighted between tracking errors of NEW and ETDC.

Composition of chapter 5 is as follows. Chapter 5.1, the robot system is explained in terms of hardware and software. Chapter 5.2 shows NEW and ETDC being implemented with same gains: $\bar{M}$, K_D, and K_P. Chapter 5.3 shows the characteristics of NEW when characteristic gain in NEW changes. Chapter 5.4, NEW and ETDC are implemented in the 6 DOF robot: FARAMAN AT2. Chapter shows the conclusion on above experimentations.

5.1 Composition of System

AT2 robot with 6 DOF is shown in figure 5.1. Motor driver and industrial computer for controlling the robot are shown in figure 5.2 and figure 5.3 respectively. And then, overall structure of system is described in figure 5.4. Specification of this robot is represented in terms of mechanical and electrical characteristics in table 5.1.

Industrial computer is included Fedora Core 5, Real Time Application Interface (RTAI)-3.4-CV, and Linux Kernel 2.6.17. Here, Fedora Core 5 is not real time operating software. Therefore, Fedora is combined with RTAI to become a real time operating system.
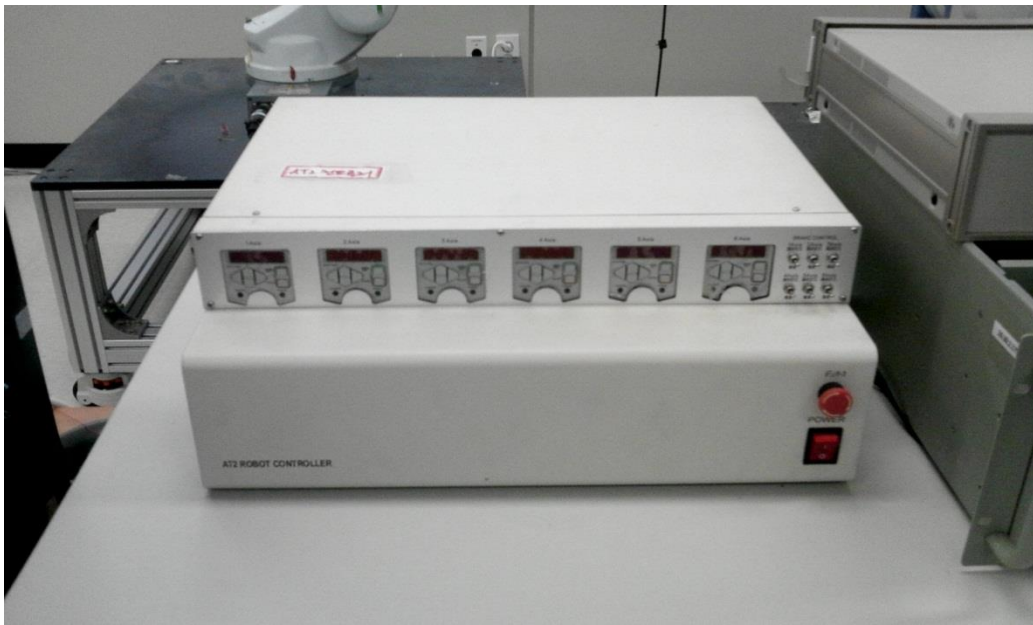

Fig. 5.1 Six degree of freedom robot: FARAMAN AT2

Fig. 5.2 Motor driver: CSD 3 series
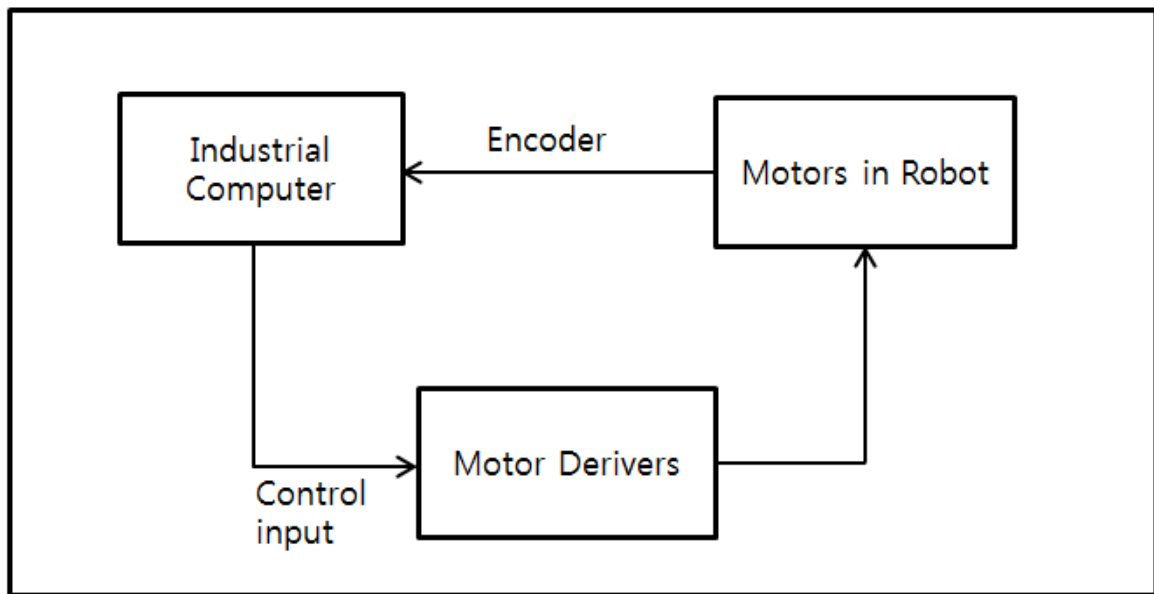

Fig. 5.3 Industrial computer

Fig. 5.4 Overall structure of the robot system

Items		Specifications
Robot type		Vertical Articulated Robot
Degree of Freedom		6
Allowed weight		3kgf
Repetition Accuracy		±0.04mm
ARM length (MAX)		720mm
Operating range & Max velocity	Joint 1	±160°(240°/s)
	Joint 2	+150° ~ -45°(240°/s)
	Joint 3	+80° ~ -200°(240°/s)
	Joint 4	±200°(320°/s)
	Joint 5	±120°(300°/s)

	Joint 6	±360°(480°/s)
	Joint 4	8.17N.m
Allowed Moment	Joint 5	8.8N.m
	Joint 6	6.36N.m
Motor type		AC servo motor
Encoder type		Absolute encoder
	Temperature	0 ~+40°C
Installation Environment	Humidity	20 ~80%RH
	Vibration	Below 0.5G
	BODY	Approx. 34kg
Weight	CONTROLLER	Approx. 25kg
CONTROLLER TYPE		SRCP Series
Power Consumption		1.6KVA

Table 5.1 Specification of FARAMAN AT2 robot

5.2 First Experimentation: NEW and ETDC with same gains

The results of frequency response characteristics of NEW were discussed in chapter 3. In

the results, NEW is shown that robustness of NEW is better than ETDC in terms of the error in the

high frequency range. However, ETDC's errors in low frequency range are less than the NEW. Hence,

NEW and ETDC with same gains such as $\bar{M}$, K_D, and K_P will be implemented at joint six in AT2

robot. And, the results of experimentation will be described with results of the frequency response characteristics analysis.

5.2.1 Implementation

ETDC is designed to be implemented for joint six in AT2 robot as follows:

$$\tau_{(t)} = \tau_{(t-L)} - \bar{M}\ddot{\theta}_{(t-L)} + \bar{M}\big[\ddot{\theta}_d + K_D\big(\dot{\theta}_d - \dot{\theta}\big) + K_P(\theta_d - \theta)\big] + \Delta H_{(t-L)} \tag{5.1}$$

$$\Delta H_{(t-L)} = \bar{M}\big[\big(\ddot{\theta}_{d(t-L)} - \ddot{\theta}_{(t-L)}\big) + K_D\big(\dot{\theta}_{d(t-L)} - \dot{\theta}_{(t-L)}\big) + K_P\big(\theta_{d(t-L)} - \theta_{(t-L)}\big)\big] + \Delta H_{(t-2L)}$$

NEW is designed as follows:

$$\tau_{(t)} = \tau_{(t-L)} - \bar{M}\ddot{\theta}_{(t-L)} + \bar{M}\big[\ddot{\theta}_d + K_D\big(\dot{\theta}_d - \dot{\theta}\big) + K_P(\theta_d - \theta)\big] + K_C\Delta H_{(t-L)} \tag{5.2}$$

$$\Delta H_{(t-L)} = \bar{M}\big[\big(\ddot{\theta}_{d(t-L)} - \ddot{\theta}_{(t-L)}\big) + K_D\big(\dot{\theta}_{d(t-L)} - \dot{\theta}_{(t-L)}\big) + K_P\big(\theta_{d(t-L)} - \theta_{(t-L)}\big)\big] + \Delta H_{(t-2L)}$$

The values of $\bar{M}$, K_D, and K_P for both NEW and ETDC are set to 0.0008, 20, and 100 respectively.

The characteristic gain K_C in NEW is set as 0.1. In PD gain, natural frequency is $10\,[\text{rad/sec}]$ and critical damping is used. Also, time of sampling interval and time delay *L* are set as 0.002 [sec] respectively.

Desired trajectory is described by using fifth-order polynomial trajectory generation scheme [2] as follows:

$$\theta_d(t) = a_0 + a_1 t + a_2 t^2 + a_3 t^3 + a_4 t^4 + a_5 t^5 \qquad (5.3)$$

$$a_0 = \theta_0,$$

$$a_1 = \dot{\theta}_0,$$

$$a_2 = \frac{\ddot{\theta}_0}{2},$$

$$a_3 = \frac{20\theta_f - 20\theta_0 - (8\dot{\theta}_f + 12\dot{\theta}_0)t_f - (3\ddot{\theta}_0 - \ddot{\theta}_f)t_f^2}{2t_f^3},$$

$$a_4 = \frac{30\theta_0 - 30\theta_f + (14\dot{\theta}_f + 16\dot{\theta}_0)t_f + (3\ddot{\theta}_0 - 2\ddot{\theta}_f)t_f^2}{2t_f^4},$$

$$a_5 = \frac{12\theta_f - 12\theta_0 - (6\dot{\theta}_f + 6\dot{\theta}_0)t_f - (\ddot{\theta}_0 - \ddot{\theta}_f)t_f^2}{2t_f^5}.$$

Where θ_0 is the initial value of angle. θ_f is the final value of angle and t_f is finish time.

Then, each value of parameters in equation (5.3) is shown in table 5.2.

Parameters / Time [sec]	θ_0 [Degree]	θ_f [Degree]	t_f [sec]
$0 < t \le 1$	0	30	1
$1 < t \le 2$	30	0	2
$2 < t \le 3$	0	-30	3
$3 < t \le 4$	-30	0	4

Table 5.2 Parameters of desired trajectory in first experimentation

5.2.2 Results

The left side of figure 5.5 shows the desired trajectory for this experimentation. The highest position is positive 30 degrees at 1 [sec] and the lowest position is negative 30 degrees at 2 [sec]. The right side of figure 5.5 represents the desired velocity. The fastest velocity is about positive 56 [degrees/sec] at 0.5 and 3.5 [sec]. The slowest velocity is about negative 56 [degrees/sec] at 1.5 and 2.5 [sec].

Figure 5.6shows the results of tracking errors when ETDC and NEW are implemented at joint six of

AT2 robot. In the figure, when NEW is compared with ETDC in terms of the errors of relatively high

frequency, frequency range of the errors in NEW is relatively less than ETDC. This phenomenon is

similar to the results of frequency response characteristic described in chapter 3. The range of

general errors in NEW is wider than ETDC. This result is similar with experimentation of ETDC and

TDC. Cause of the result is related with the characteristic gain in NEW because the gain is set to 0.1

to be close to the characteristic of TDC. Hence, this experimentation properly shows the characteristic

of NEW and ETDC compared in frequency response characteristics analysis.
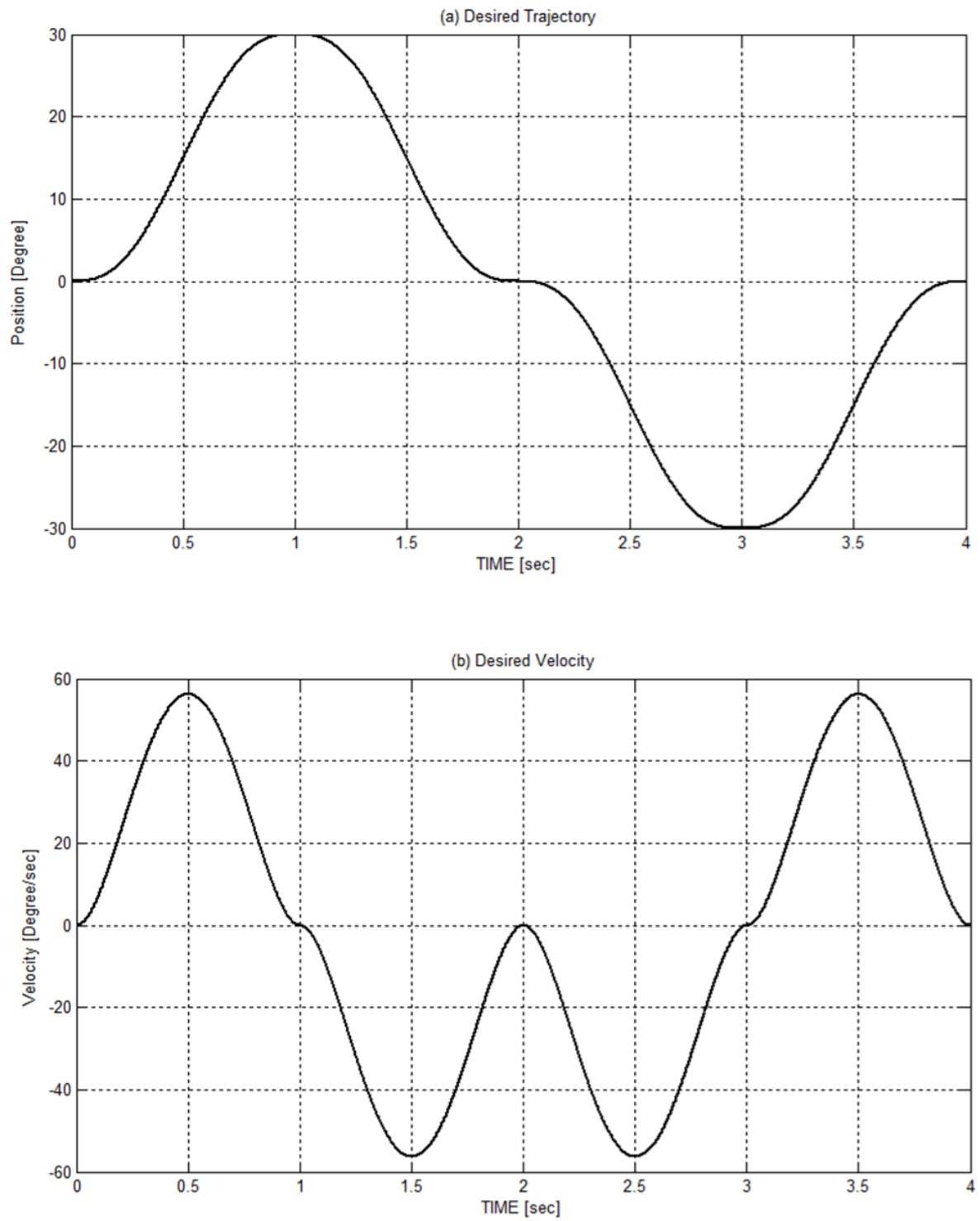
Fig. 5.5 Desired input for first experimentation: (a) desired trajectory (b) desired velocity
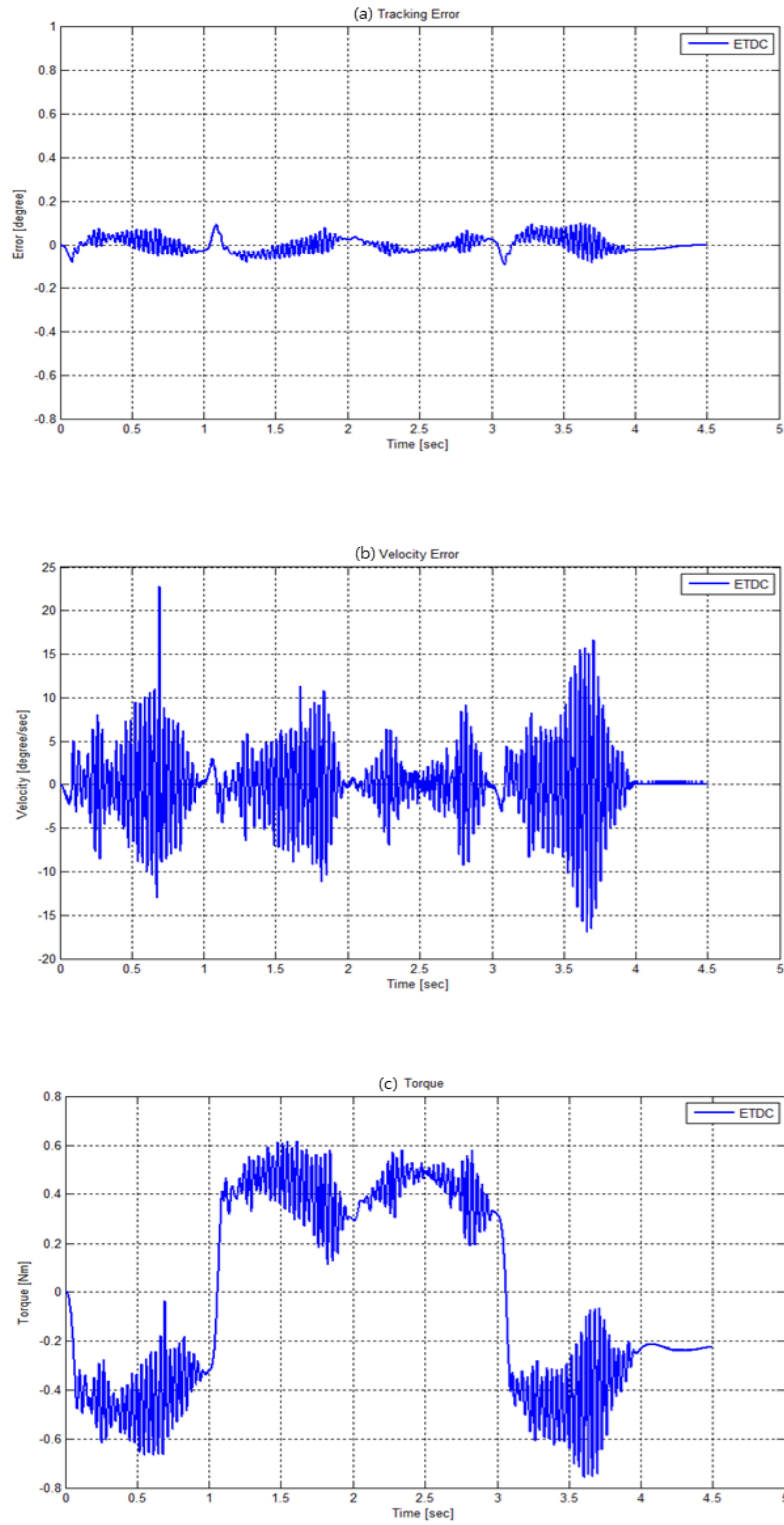
Fig. 5.6 Results of ETDC in first experimentation:

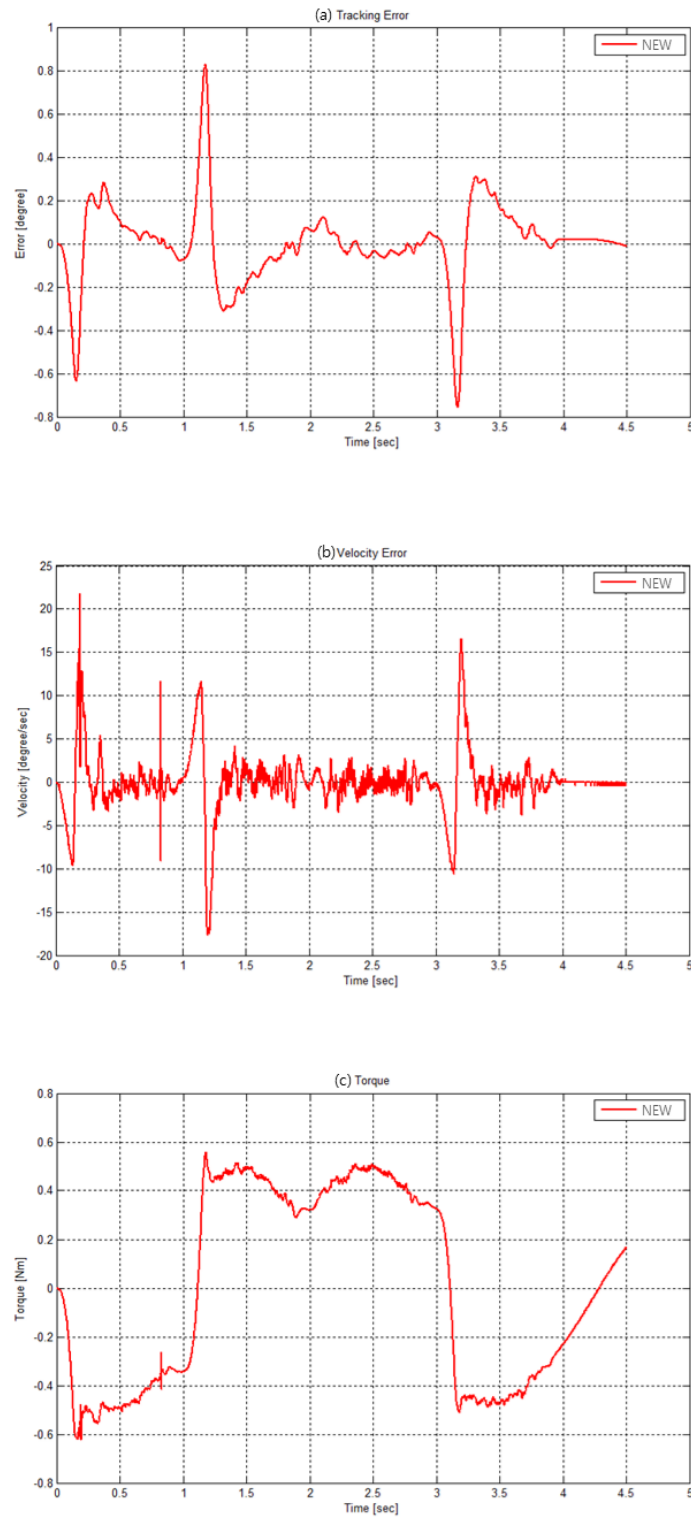(a) tracking error at joint 6 (b) velocity error at joint 6 (c) torque at joint 6

Fig. 5.7 Results of NEW in first experimentation:

(a) tracking error at joint 6 (b) velocity error at joint 6 (c) torque at joint 6

5.3 Second Experimentation: NEW with various characteristic gains

This experimentation shows the effect of the characteristic gain of NEW. Range of the gain is

defined between 0 and 1. Here, when the gain is increased to be closer to 1 from 0.1. NEW is

implemented at joint six in AT2 like the previous experimentation. The results of this experimentation

are analyzed in terms of control performance and the noise including chattering problems.

5.3.1 Implementation

NEW is designed for this experimentation as follows:

$$\tau_{(t)} = \tau_{(t-L)} - \bar{M}\ddot{\theta}_{(t-L)} + \bar{M}[\ddot{\theta}_d + K_D(\dot{\theta}_d - \dot{\theta}) + K_P(\theta_d - \theta)] + K_C\Delta H_{(t-L)} \qquad (5.4)$$

$$\Delta H_{(t-L)} = \bar{M}[(\ddot{\theta}_{d(t-L)} - \ddot{\theta}_{(t-L)}) + K_D(\dot{\theta}_{d(t-L)} - \dot{\theta}_{(t-L)}) + K_P(\theta_{d(t-L)} - \theta_{(t-L)})] + \Delta H_{(t-2L)}$$

Parameters of NEW are described in table 5.3.

$\bar{M}$, K_D, and K_P in NEW used same values decided in the previous experimentation. In PD gain,

natural frequency is $10\,[\mathrm{rad/sec}]$ and critical damping is used. The gain K_C is increased from 0.1 to

1.0. Also, the time of sampling interval and the time delay *L* are both set to 0.001 [sec].

Case Parameters	1	2	3	4	5
$\bar{M}$	0.0008	0.0008	0.0008	0.0008	0.0008
K_D	20	20	20	20	20
K_P	100	100	100	100	100
K_C	0.1	0.3	0.5	0.7	0.9

Table 5.3 Parameters of NEW in second experimentation

Desired trajectory is described by using fifth-order polynomial trajectory generation scheme [2] as follows:

$$\theta_d(t) = a_0 + a_1 t + a_2 t^2 + a_3 t^3 + a_4 t^4 + a_5 t^5 \tag{5.5}$$

$$a_0 = \theta_0,$$

$$a_1 = \dot{\theta}_0,$$

$$a_2 = \frac{\ddot{\theta}_0}{2},$$

$$a_3 = \frac{20\theta_f - 20\theta_0 - (8\dot\theta_f + 12\dot\theta_0)t_f - (3\ddot\theta_0 - \ddot\theta_f)t_f^2}{2t_f^3},$$

$$a_4 = \frac{30\theta_0 - 30\theta_f + (14\dot\theta_f + 16\dot\theta_0)t_f + (3\ddot\theta_0 - 2\ddot\theta_f)t_f^2}{2t_f^4},$$

$$a_5 = \frac{12\theta_f - 12\theta_0 - (6\dot\theta_f + 6\dot\theta_0)t_f - (\ddot\theta_0 - \ddot\theta_f)t_f^2}{2t_f^5}.$$

Where θ_0 is the initial value of angle. θ_f is the final value of angle and t_f is finish time.

Then, each value of parameters in equation (5.5) is shown in table 5.2.

Parameters Time [sec]	θ_0 [Degree]	θ_f [Degree]	t_f [sec]
$0 < t \leq 1.5$	0	30	1.5
$1.5 < t \leq 3$	30	0	3
$3 < t \leq 4.5$	0	-30	4.5
$4.5 < t \leq 6$	-30	0	6

Table 5.4 Parameters of desired trajectory in second experimentation

5.3.2 Results

Figure 5.8 shows the desired trajectory for this experimentation. The highest position is positive 30

degrees at 1 [sec] and the lowest position is negative 30 degrees at 2 [sec]. Figure 5.9 shows the

results of tracking errors when the characteristic gain is increased from 0.1 to 0.9. In the results, when

the gain is 0.1, peak point in positive error range is close to about 0.49. When the gain is 0.3, peak

point in positive error range is close to about 0.25. When the gain is 0.7, peak point in positive error

range is close to about 0.1. From above results, when the gain increases, overall range of the errors

is decreased. However, when the gain increases, frequency of errors including chattering is also
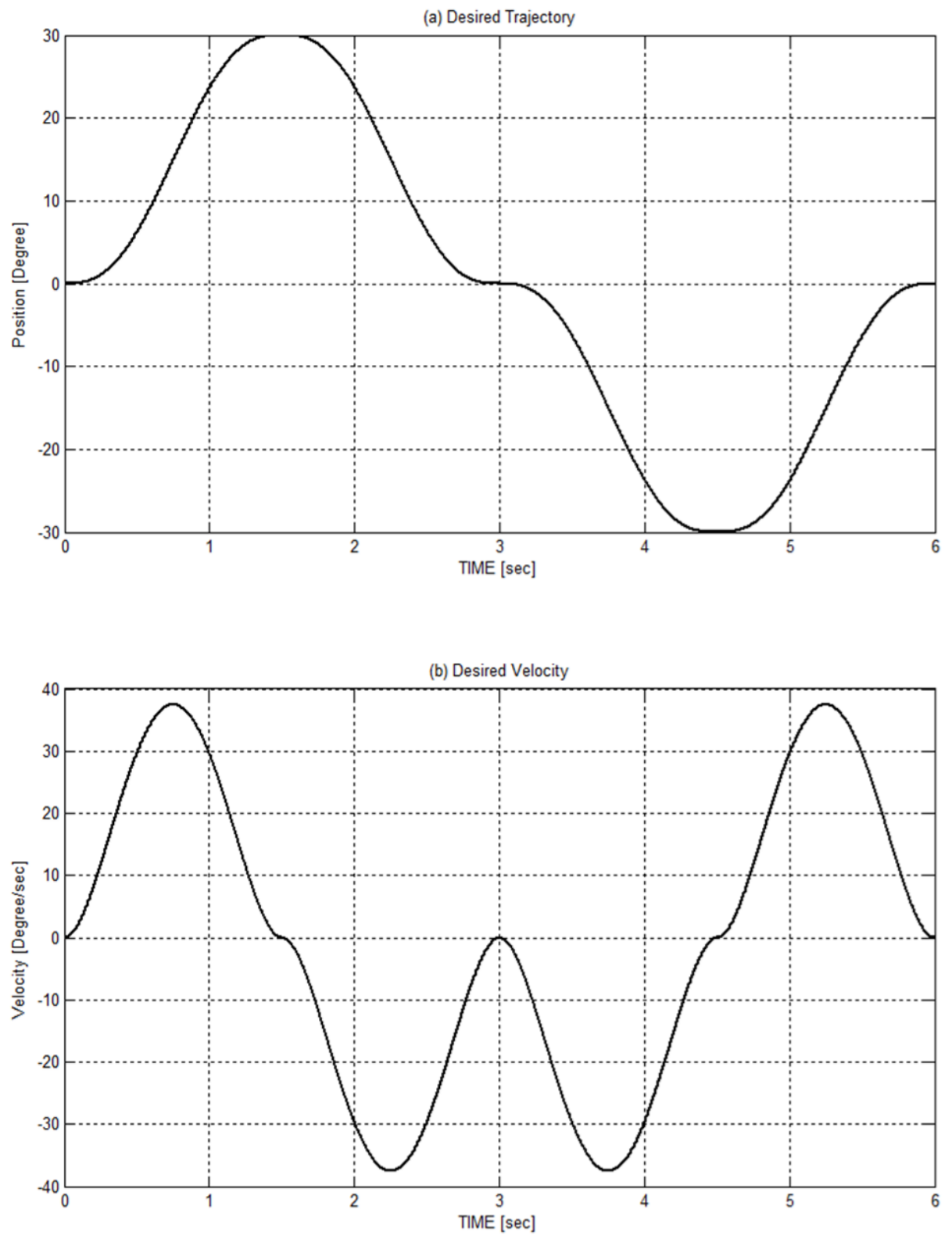
increased.

Fig. 5.8 Desired input for second experimentation: (a) desired trajectory (b) desired velocity
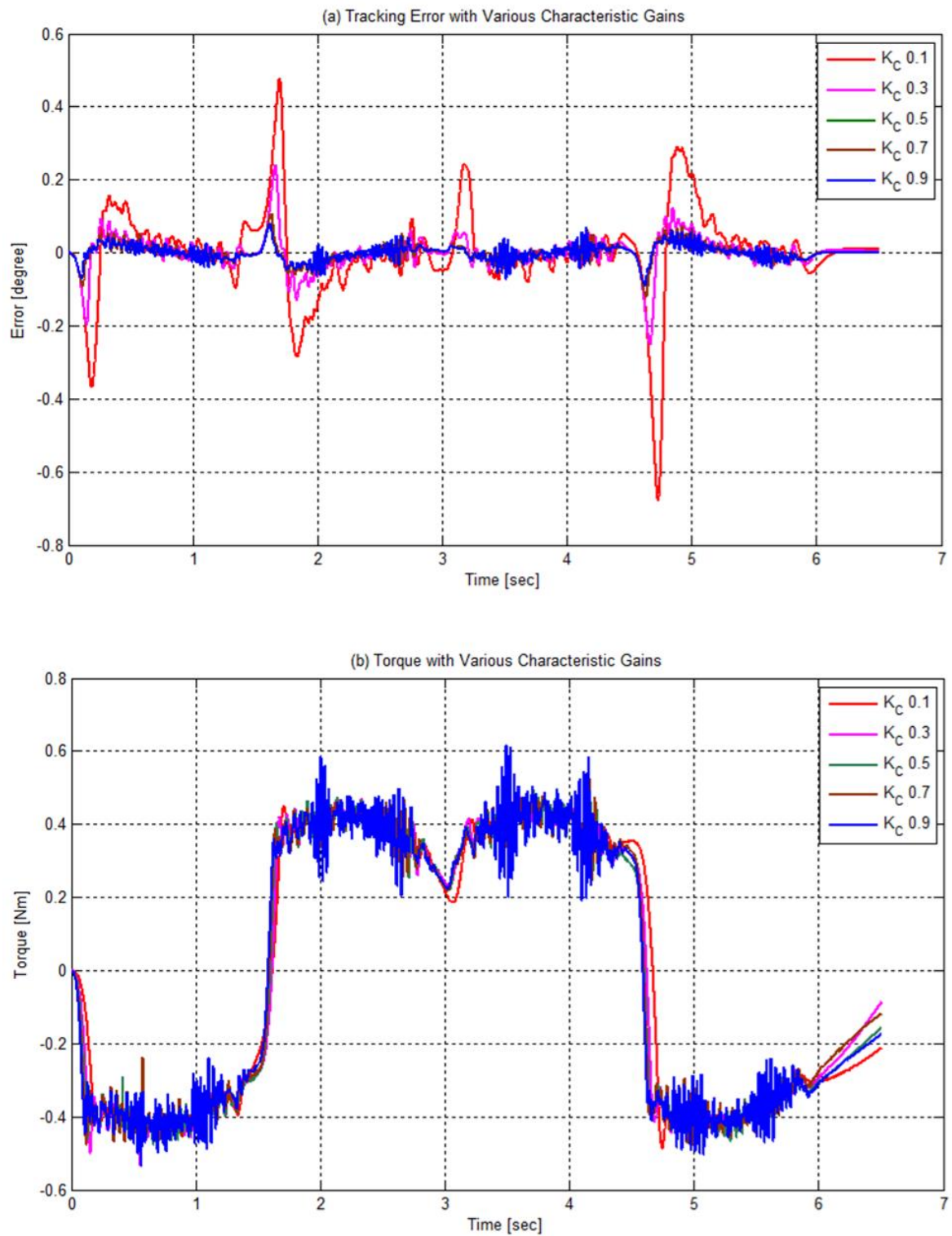
Fig. 5.9 Results of NEW in second experimentation:

(a) tracking error with various characteristic gains (b) torque with various characteristic gains

5.4 Third Experimentation: NEW and ETDC with optimally tuned gains

This experimentation shows the comparison results of control performance in each controller

when the gains of NEW and ETDC are optimally tuned. NEW and ETDC are implemented for six

joints in AT2 robot. The results of this experimentation are analyzed in terms of control performance.

5.4.1 Implementation

ETDC is designed to implement in AT2 robot as follows:

$$\boldsymbol{\tau}_{(t)} = \boldsymbol{\tau}_{(t-L)} - \bar{\mathbf{M}}\ddot{\boldsymbol{\theta}}_{(t-L)} + \bar{\mathbf{M}}\big[\ddot{\boldsymbol{\theta}}_{\mathbf{d}(t)} + \mathbf{K_D}\big(\dot{\boldsymbol{\theta}}_{\mathbf{d}(t)} - \dot{\boldsymbol{\theta}}_{(t)}\big) + \mathbf{K_P}\big(\boldsymbol{\theta}_{\mathbf{d}(t)} - \boldsymbol{\theta}_{(t)}\big)\big] + \Delta\mathbf{H}_{(t-L)} \qquad (5.6)$$

$$\Delta\mathbf{H}_{(t-L)} = \bar{\mathbf{M}}\big[\big(\ddot{\boldsymbol{\theta}}_{\mathbf{d}(t-L)} - \ddot{\boldsymbol{\theta}}_{(t-L)}\big) + \mathbf{K_D}\big(\dot{\boldsymbol{\theta}}_{\mathbf{d}(t-L)} - \dot{\boldsymbol{\theta}}_{(t-L)}\big) + \mathbf{K_P}\big(\boldsymbol{\theta}_{\mathbf{d}(t-L)} - \boldsymbol{\theta}_{(t-L)}\big)\big] + \Delta\mathbf{H}_{(t-2L)}$$

Here, $\bar{\mathrm{M}}$ is 6 by 6 diagonal matrix and tuned from a tiny value. The value is described in table 5.5. In

PD gain, the natural frequency is $10\,[\mathrm{rad/sec}]$ with critical damping. $\mathrm{K_D}$ and $\mathrm{K_P}$ are set 20 and 100

respectively. Also, time of sampling interval and value of time delay are set as 0.002 [sec] respectively.

And, NEW is designed as follows:

$$\mathbf{\tau}_{(t)} = \mathbf{\tau}_{(t-L)} - \mathbf{\bar{M}}\mathbf{\ddot{\theta}}_{(t-L)} + \mathbf{\bar{M}}[\mathbf{\ddot{\theta}}_{\mathbf{d}(t)} + \mathbf{K_D}(\mathbf{\dot{\theta}}_{\mathbf{d}(t)} - \mathbf{\dot{\theta}}_{(t)}) + \mathbf{K_P}(\mathbf{\theta}_{\mathbf{d}(t)} - \mathbf{\theta}_{(t)})] + \mathbf{K_C}\Delta\mathbf{H}_{(t-L)} \qquad (5.7)$$

$$\Delta\mathbf{H}_{(t-L)} = \mathbf{\bar{M}}[(\mathbf{\ddot{\theta}}_{\mathbf{d}(t-L)} - \mathbf{\ddot{\theta}}_{(t-L)}) + \mathbf{K_D}(\mathbf{\dot{\theta}}_{\mathbf{d}(t-L)} - \mathbf{\dot{\theta}}_{(t-L)}) + \mathbf{K_P}(\mathbf{\theta}_{\mathbf{d}(t-L)} - \mathbf{\theta}_{(t-L)})] + \Delta\mathbf{H}_{(t-2L)}$$

In parameters, values of $\bar{M}$, K_D, K_P, and K_C are shown in table 5.6. Here, K_C is 6 by 6 diagonal

matrix and values of K_C is used as 0.1. NEW also used same natural frequency and critical damping

as ETDC. Also, the time of sampling interval and time delay *L* are both set to 0.002 [sec] respectively.

	Joint 1	Joint 2	Joint 3	Joint 4	Joint 5	Joint 6
$\bar{M}$	0.0048	0.0041	0.0062	0.0042	0.00148	0.00075
K_D	20	20	20	20	20	20
K_P	100	100	100	100	100	100

Table 5.5 Parameters of ETDC in third experimentation

	Joint 1	Joint 2	Joint 3	Joint 4	Joint 5	Joint 6
$\bar{\mathrm{M}}$	0.032	0.028	0.035	0.031	0.0118	0.0062
$\mathrm{K_D}$	20	20	20	20	20	20
$\mathrm{K_P}$	100	100	100	100	100	100
$\mathrm{K_C}$	0.1	0.1	0.1	0.1	0.1	0.1

Table 5.6 Parameters of NEW in third experimentation

Desired trajectory is described by using fifth-order polynomial trajectory generation scheme [2] as

follows:

$$\theta_d(t) = a_0 + a_1 t + a_2 t^2 + a_3 t^3 + a_4 t^4 + a_5 t^5 \tag{5.8}$$

$$a_0 = \theta_0,$$

$$a_1 = \dot{\theta}_0,$$

$$a_2 = \frac{\ddot{\theta}_0}{2},$$

$$a_3 = \frac{20\theta_f - 20\theta_0 - (8\dot{\theta}_f + 12\dot{\theta}_0)t_f - (3\ddot{\theta}_0 - \ddot{\theta}_f)t_f^2}{2t_f^3},$$

$$a_4 = \frac{30\theta_0 - 30\theta_f + (14\dot{\theta}_f + 16\dot{\theta}_0)t_f + (3\ddot{\theta}_0 - 2\ddot{\theta}_f)t_f^2}{2t_f^4},$$

$$a_5 = \frac{12\theta_f - 12\theta_0 - (6\dot{\theta}_f + 6\dot{\theta}_0)t_f - (\ddot{\theta}_0 - \ddot{\theta}_f)t_f^2}{2t_f^5}.$$

Where θ_0 is the initial value of angle. θ_f is the final value of angle, and t_f is the finish time.

Here, AT2 robot has 6 DOF. Therefore, each joint trajectory is set as θ_d. It means that 6 joints follow

the same trajectory: $\theta_d = \theta_{d1} = \theta_{d2} = \theta_{d3} = \theta_{d4} = \theta_{d5} = \theta_{d6}$.

Then, each value of parameters in equation (5.8) is shown in table 5.6.

Parameters Time [sec]	θ_0 [Degree]	θ_f [Degree]	t_f [sec]
$0 < t \leq 2$	0	30	2
$2 < t \leq 4$	30	0	4
$4 < t \leq 6$	0	-30	6
$6 < t \leq 8$	-30	0	8

Table 5.7 Desired values of trajectory in third experimentation

5.4.2 Results

In figure 5.10, the graph (a) shows desired trajectory for this experimentation. The highest position is positive 30 degrees at 2 [sec] and the lowest position is negative 30 degrees at 6 [sec]. The graph (b) shows desired velocity. The fastest velocity is about positive 28 [degrees/sec] at 1 and 7 [sec]. The slowest velocity is about negative 28 [degrees/sec] at 3 and 5 [sec]. Results of tracking errors of ETDC are plotted in figure 5.11. In the figure, the graph (a), (b), (c), (d), (e), and (f) are tracking errors at joint 1, 2, 3, 4, 5, and 6 respectively. Figure 5.12 represents the torque of each joint in AT2 robot when ETDC is applied. Results of tracking errors in NEW are plotted in figure 5.13. In the figure, the graph (a), (b), (c), (d), (e), and (f) are tracking errors at joint 1, 2, 3, 4, 5, and 6 respectively. Figure 5.14 represents the torque of each joint in AT2 robot when NEW is applied. ETDC is compared with NEW in terms of errors including chattering. NEW shows that robustness against the relatively high frequency errors is better than ETDC. Especially, in joint 4 of figure 5.11 and 5.13, NEW shows more enhanced performance than ETDC in terms of the noise like chattering problems and the general range of the errors respectively. When NEW's error like the spike in early part of tracking error

graph shown in figure 5.13 is compared with ETDC's error in figure 5.11, the error of NEW is generally

less than ETDC. NEW error reduction is evident by figure 5.11 and 5.13. When the error at joint 4 in

figure 5.11 (-0.038) is compared to the error at joint 4 in figure 5.13 (-0.047). The comparison reveals

that error reduction of NEW over ETDC is about 19%. Therefore, NEW is generally better than ETDC
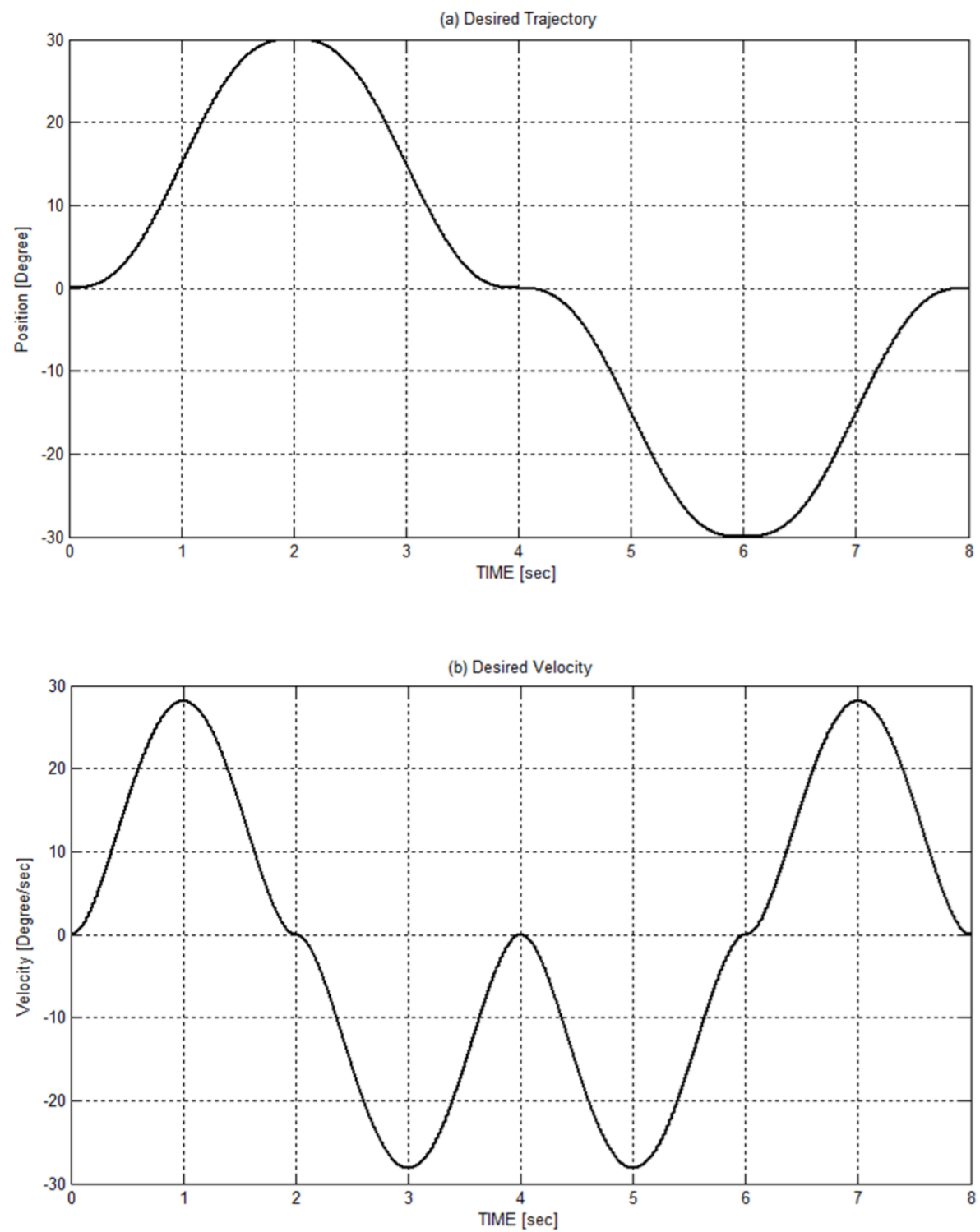
in terms of initial error.

Fig. 5.10 Desired input for third experimentation: (a) desired trajectory (b) desired velocity
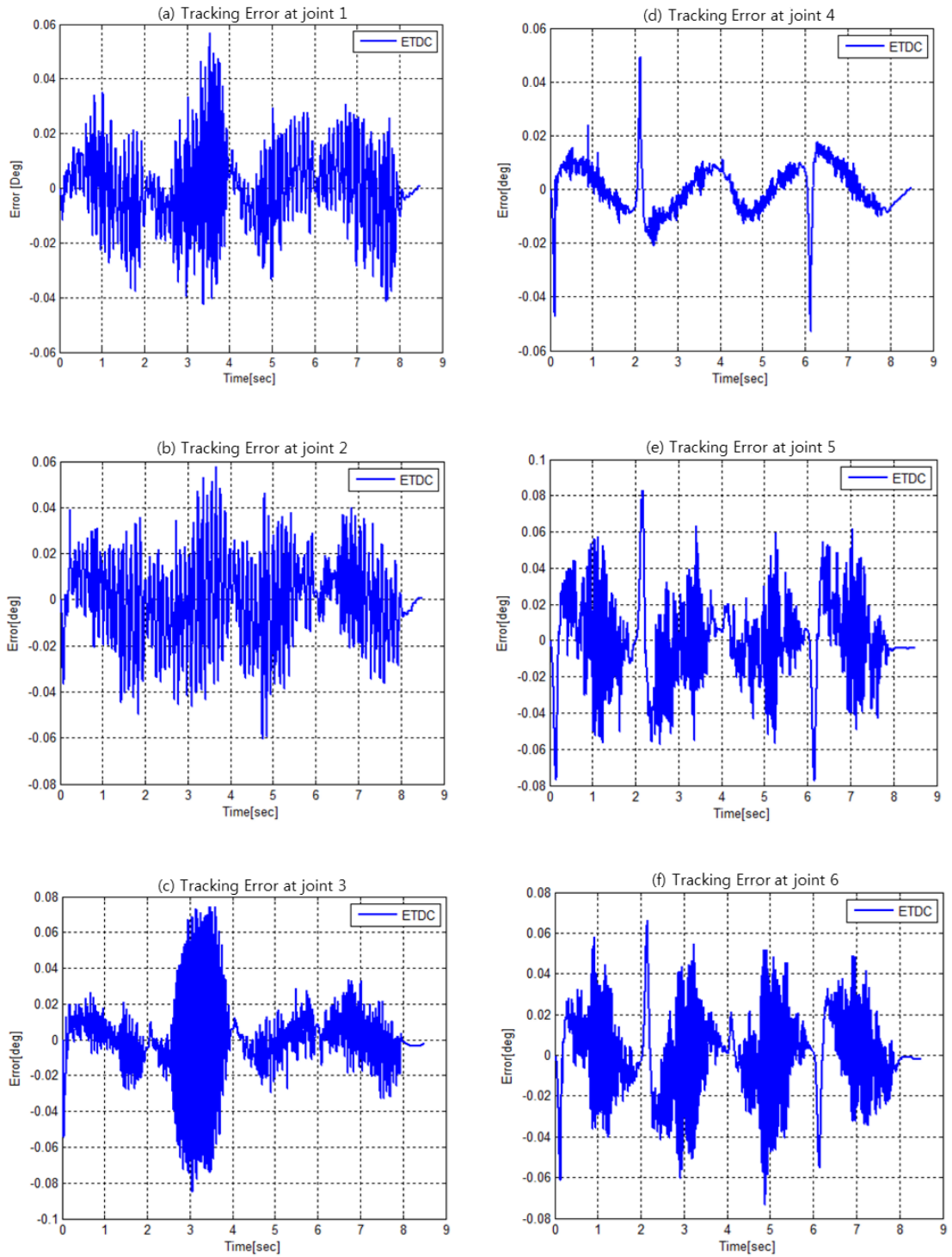
Fig. 5.11 Tracking errors of ETDC in third experimentation:

(a) tracking error at joint 1 (b) tracking error at joint 2 (c) tracking error at joint 3

(d) tracking error at joint 4 (e) tracking error at joint 5 (f) tracking error at joint 6
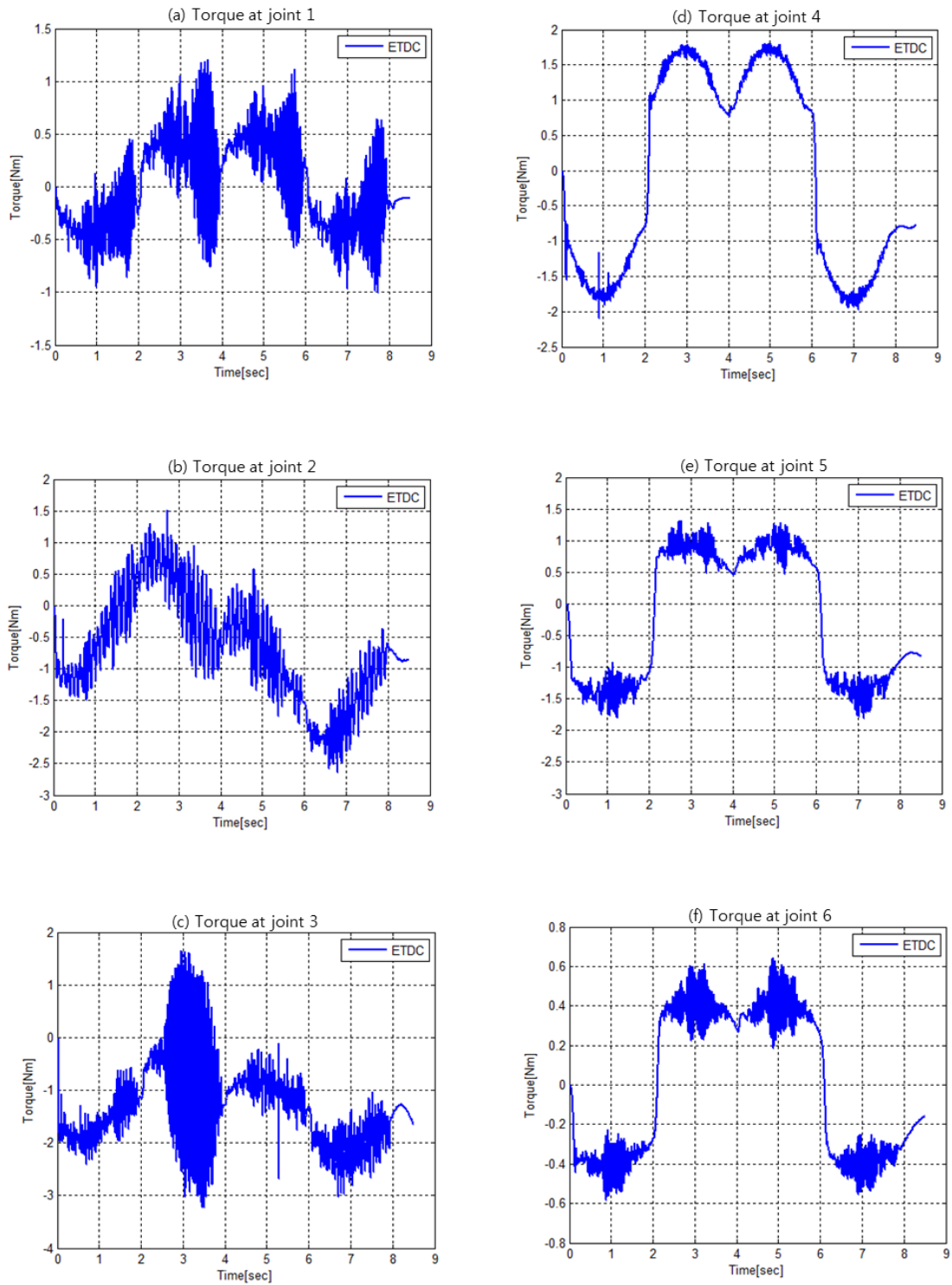
Fig. 5.12 Torque of ETDC in third experimentation:

(a) torque at joint 1 (b) torque at joint 2 (c) torque at joint 3

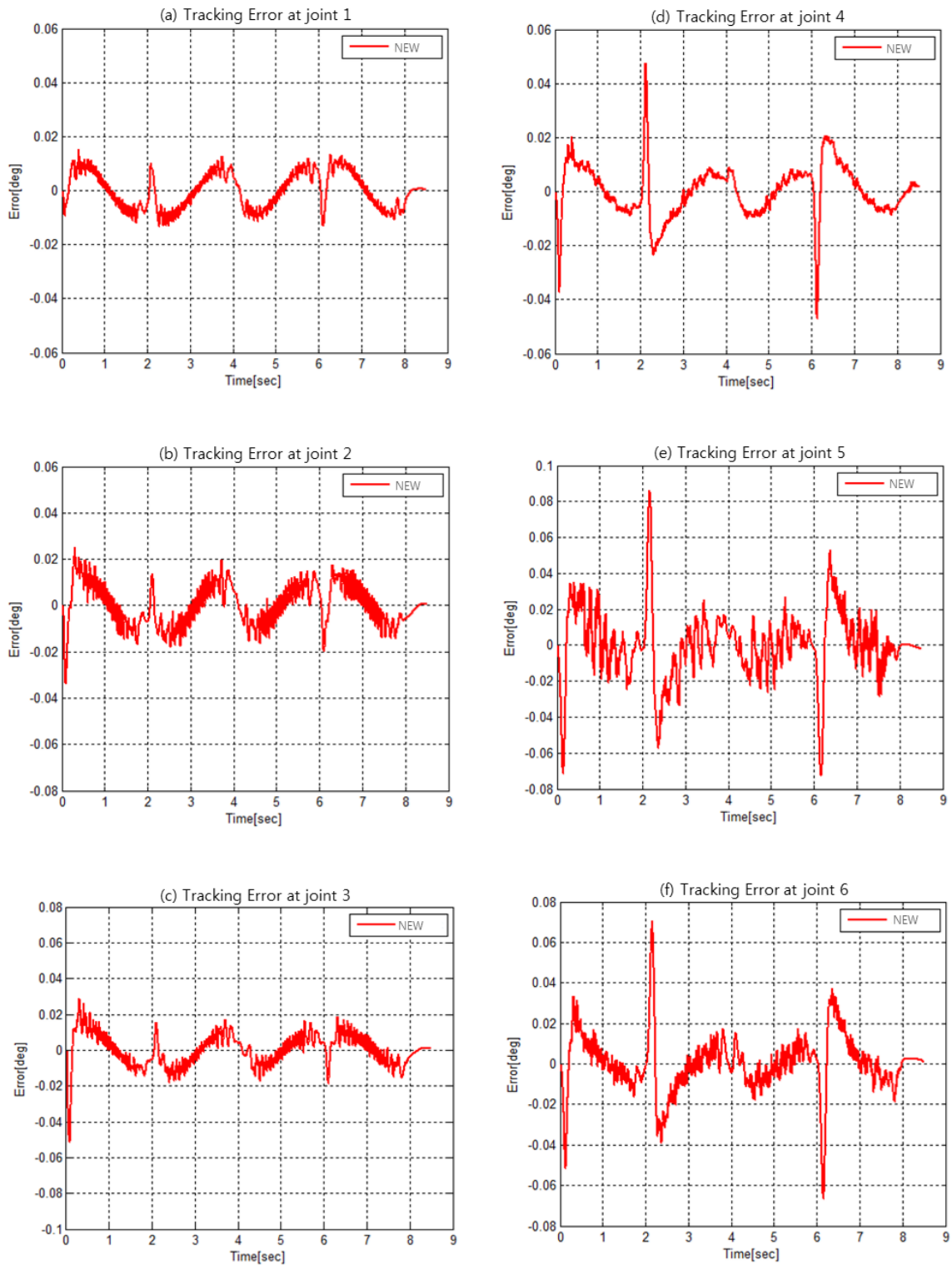(d) torque at joint 4 (e) torque at joint 5 (f) torque at joint 6

Fig. 5.13 Tracking errors of NEW in third experimentation:

(a) tracking error at joint 1 (b) tracking error at joint 2 (c) tracking error at joint 3

(d) tracking error at joint 4 (e) tracking error at joint 5 (f) tracking error at joint 6
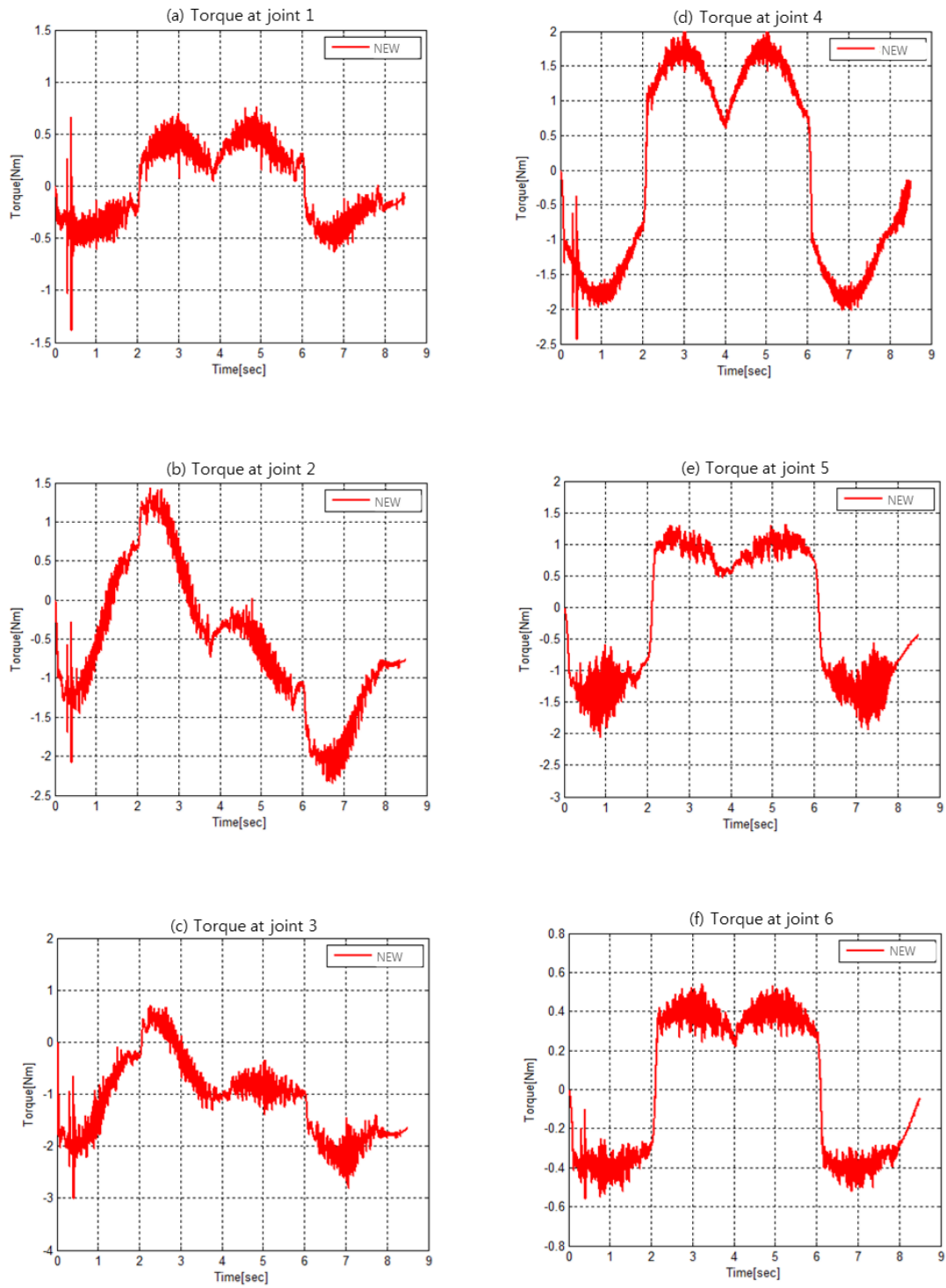
Fig. 5.14 Torque of NEW in third experimentation:

(a) torque at joint 1 (b) torque at joint 2 (c) torque at joint 3

(d) torque at joint 4 (e) torque at joint 5 (f) torque at joint 6

5.5 Conclusion

In this chapter, three experimentations are shown to check the characteristic of NEW and verify control performance of NEW by comparing ETDC. In the first experimentation, parameters of NEW are same with parameters of ETDC except the characteristic gain of NEW because the gain is not included in ETDC. Also, this experimentation properly explains the characteristic of NEW and ETDC compared in frequency response characteristics analysis in chapter 3.

In the second experimentation, effects of the characteristic gain in NEW are shown when the gain is increased from 0.1 to 1.0. Overall range of the errors is decreased in the results. However, the errors like chattering problems are increased because characteristic of NEW is close to ETDC when the gain is close to one.

In the third experimentation, NEW and ETDC are optimally tuned to show best performance of the controllers. In the results, NEW is more robust than ETDC in terms of the errors including chattering. Also, NEW generally shows better performance than ETDC in terms of the overall range of the errors and the initial error respectively.

From above results, NEW's control performance is more enhanced than control performance of

ETDC.

VI . Conclusion

Robust Control techniques are one of several control schemes used to control plants with modeling errors or model uncertainty to follow desired dynamic behavior. One type of robust controller is Time Delay Control (TDC) [C] for robot manipulators. TDC uses Time Delay Estimation (TDE) scheme to estimate the uncertainty of models such as disturbances and unknown dynamics. However, control performance of TDC is degraded by TDE errors. Hence, an advanced research, Enhanced Time Delay Control (ETDC) was developed by J. Y. Park and P. H. Chang in 2003 [A]. ETDC are more accurate than TDC at the same sampling frequency.

ETDC shows better performance than TDC in the experimentation of a real system because ETDC complements TDE errors in TDC. In comparing the advantages of TDC and ETDC, TDC is relatively more robust in terms of noise including chattering. ETDC generally shows better performance in terms of range of the tracking error than TDC.

In order to alleviate the problems exhibited by ETDC, An Enhanced Time-Delay Control using a

Second-Order Time-Delay Estimation (NEW) is proposed. The new controller is based on ETDC.

Therefore, ETDC is analyzed in terms of different points between ETDC and TDC. Different point is

the TDE error term, and, the TDE error term in ETDC is analyzed. The term constantly accumulates

with previous TDE error term. In the analysis of frequency response characteristic of ETDC and TDC,

ETDC shows that the robustness of ETDC is better than TDC in terms of the errors in low frequency

range when TDE error is given as an input. However, in high frequency range, ETDC's errors show

rapid fluctuation like an unstable state.

NEW contains the TDE error term derived in equation (2.22) to alleviate TDE errors when TDE

scheme is applied. And, the TDE error term in NEW combines with a certain gain. The gain is called

characteristic gain. By adding the gain, NEW can control values of TDE error term. Characteristics of

NEW are determined by tuning the characteristic gain in NEW. When the gain is close to zero, NEW

shows the characteristics of TDC. But, when the gain is close to one, NEW exhibits characteristics of

ETDC. The analysis of the frequency response characteristic, the characteristic gain in NEW is tuned

to 0.1. Consequently, NEW shows that robustness of NEW is better than ETDC in high frequency

range.

 In the three experimentations, NEW's control performance is shown by comparing ETDC's control

performance. In the first experimentation, NEW uses the same parameters as the ETDC, except for

the characteristic gain in NEW. The experimentation verified the frequency response characteristic of

NEW and ETDC. The second experimentation shows the effects of the characteristic gain of NEW.

Overall range of the errors of NEW decreases when the gain is increased from 0.1 to 1.0. However,

errors including chattering are increased because the characteristic of NEW is closer to ETDC when

the gain is close to one. In the third experimentation, the gains of NEW and ETDC are both optimally

tuned to show best performances. NEW is more robust than ETDC in terms of the errors including

chattering. Also, NEW generally shows better performance than ETDC in terms of the overall range of

the errors and the initial error.

From above results, the proposed controller's effectiveness is verified. When NEW is applied to

various real systems for precision control, NEW shows usefulness in terms of range of errors, noise

including chattering, and initial error.

.

.

Reference

[1] J. Y. Park and P. H. Chang "Enhanced Time Delay Control and Its Applications to Force Control of Robot Manipulators" *International journal of HWRS,* Vol. 4, No.2 pp. 44-50 June 2003.

[2] John J. Craig (2005). Introduction to robotics, PEARSON, USA, 201 pages.

[3] K. Youcef-Toumi, and C. C. Shortlidge, "Control of Robot Manipulators using Time Delay", *IEEE Int, Conference on Robotics and Automations*, 1991

[4] K. Youcef-Toumi, and O. lto, "A Time Delay Controller for systems with Unknown Dynamics", *ASME Journal of Dynamics Systems, Measurement, and Control*, Vol. 112, pp. 133-142, Mar. 1990

[5] K. Youcef-Toumi, and S-T Wu, "input/output Linearization Using Time Delay Control", *ASME Journal of Dynamics Systems, Measurement, and Control*, Vol. 114, pp. 10-19, Mar 1992.

[6] P. H. Chang, and J. W. Lee,,, "An Observer Design for Time-Delay Control and Its Application to DC Servomotor", *Proceedings of the American Control Conference*, pp. 1032-1036, 1993.

[7] P. H. Chang, B. S. Park, and K. C. Park, "An Experimental Study on Improving Hybrid Position/Force Control of A Robot Using Time Delay Control", *Mechatronics*, Vol. 6, No. 8, pp. 915-931, 1996.

[8] P. H. Chang. D. S. Kim, and K. C. Park "Robust Force/Position control of A Robot Manipulator Using Time-Delay Control", *Control Engineering Practice,* Vol. 3, No. 9, pp. 1255-1264, 1995.

[9] Pyung H. Chang and Suk H. Park, "The development of Anti-windup Scheme and stick-slip Compensator for Time Delay Control", *Proc. ACC*, Vol. 6, pp. 3629-3622. 1998.

[10] RUSSEL. G. MORGAN and UNIT OZGUNER, "A Decentralized Variable Structure Control Algorithm for Robotic Manipulators", *IEEE Journal of Robotics and Automation*, Vol. RA-1, No. 1. MARCH 1985.

[11] S. Q. Lee, and P. H. Chang, "Analysis and Compensation of Force Fluctuation Responses In Robot Hybrid Control Using TDC", *Proceedings of the KSME Spring Annual Meeting*, pp. 396-401. 1996

[12] T. C. Hsia, and L. S. Gao, "Robot Manipulator Control Using Decentralized Linear Time-Invariant Time-Delayed Joint Controllers", *Proceedings of the IEEE International conference on Robotics and Automation*, pp. 2070-2075, 1990.

[13] T. C. Hsia, T. A. Lasky, and Z. Y. Guo, "Robust Independent Robot Joint Control: Design and Experimentation", *Robotics and Automation, 1988. Proceedings., IEEE International Conference* Vol. 3, pp. 1329-1334 April 1988

[14] 박석호, "강한 비선형성(포화요소/마찰)을 갖는 시스템의 시간지연제어에 관한 연구", M.S thesis, 한국과학기술원, 기계공학과, 1995.

[15] 박석호, "시간지연추정과 스위칭동작의 결합을 통한 강인 제어기/관측기에 관한 연구", ph.D.thesis, 한국과학기술원 기계공학과. 2000.

[16] 이성욱, "적분형 슬라이딩 면과 시간 지연을 이용한 제어기법에 관한 연구 및 굴삭기 시스템에 적용", ph.D.thesis, 한국과학기술원, 기계공학과. 2002.

[17] 조건래, "로봇 매니퓰레이터를 위한 시간지연추정과 내부모델 개념을 결합한 강인제어기에 관현 연구", M.S thesis, 한국과학기술원, 기계공학과. 2003

Appendix A

In appendix A, transfer function of TDC is derived from TDC's error dynamics (2.12).

$$\ddot{\mathbf{e}} + \mathbf{K_D}\dot{\mathbf{e}} + \mathbf{K_P}\mathbf{e} = \bar{\mathbf{M}}^{-1}\Delta\mathbf{H}_{(t)} \tag{2.12}$$

Equation (2.12) is represented in time domain as follows:

$$\ddot{\mathbf{e}}_{(t)} + \mathbf{K_D}\dot{\mathbf{e}}_{(t)} + \mathbf{K_P}\mathbf{e}_{(t)} = \bar{\mathbf{M}}^{-1}\Delta\mathbf{H}_{(t)} \tag{A.1}$$

Laplace transform is applied to the error dynamics (A.1) with an assumption that time t is

sufficient as follows:

$$s^2\mathbf{E}(s) + \mathbf{K_D}s\mathbf{E}(s) + \mathbf{K_P}\mathbf{E}(s) = \bar{\mathbf{M}}^{-1}\Delta\mathbf{H}(s) \tag{A.2}$$

Where $\mathbf{E}(s)$ is Laplace transform of $\boldsymbol{\theta}_{\mathbf{d}(t)} - \boldsymbol{\theta}_{(t)}$: $\mathbf{e}_{(t)} \xrightarrow{\mathcal{L}} \mathbf{E}(s)$.

If each joint is individually analyzed, equation (A.2) can be described regarding arbitrary joint i

as follows:

$$(s^2 + K_{Dii}s + K_{Pii})E_i(s) = \bar{M}_{ii}^{-1}\Delta H_i(s) \tag{A.3}$$

Where $\bar{M}_{ii}$: ith diagonal element of $\bar{\mathbf{M}}$, K_{Dii}: ith diagonal element of $\mathbf{K_D}$, K_{Pii}: ith diagonal

element of $\mathbf{K_P}$, $E_i(s)$: ith element of $\mathbf{E}(s)$, and $\Delta H_i(s)$: ith element of $\Delta\mathbf{H}(s)$.

Transfer function of TDC is described from equation (A.3) as follows:

$$\frac{E_i(s)}{\Delta H_i(s)} = \frac{\bar{M}_{ii}^{-1}}{(s^2 + K_{Dii}s + K_{Pii})} \tag{A.4}$$

Appendix B

Time Delay Control (TDC) compared with Enhanced Time Delay Control (ETDC) regarding

performance of tracking error in SAMSUNG FARAMAN AT2 robot.

TDC is designed to implement in AT2 robot as follows:

$$\tau_{(t)} = \tau_{(t-L)} - \bar{M}\ddot{\theta}_{(t-L)} + \bar{M}\left(\ddot{\theta}_d + K_D(\dot{\theta}_d - \dot{\theta}) + K_P(\theta_d - \theta)\right) \tag{B.1}$$

Here, $\bar{M}$ is 6 by 6 diagonal matrix and tuned from nominal value. The values are described in

table B.1. In PD gain, natural frequency is 10 [rad/sec] with critical damping. K_D and K_P are set

20 and 100 respectively, and time of sampling interval is set to 0.002 [sec], and time delay L uses

time of sampling interval.

ETDC is designed as follows:

$$\tau = \bar{M}\left[\ddot{\theta}_d + K_D(\dot{\theta}_d - \dot{\theta}) + K_P(\theta_d - \theta)\right] + \hat{H}_{(t)} + \Delta H_{(t-L)} \tag{B.2}$$

$$\hat{H}_{(t)} = \tau_{(t-L)} - \bar{M}\ddot{\theta}_{(t-L)}$$

$$\Delta H_{(t-L)} = \bar{M}\left[\left(\ddot{\theta}_{d(t-L)} - \ddot{\theta}_{(t-L)}\right) + K_D\left(\dot{\theta}_{d(t-L)} - \dot{\theta}_{(t-L)}\right) + K_P\left(\theta_{d(t-L)} - \theta_{(t-L)}\right)\right] + \Delta H_{(t-2L)}$$

In parameters, values for $\overline{M}$, K_D, and K_P, are shown in table B.2. Here, $\overline{M}$ is 6 by 6 diagonal

matrix and tuned from nominal value. The values are described in table B.2. In PD gain, natural

frequency is 10 [rad/sec] with critical damping. K_D and K_P are set 20 and 100 respectively. Also,

sampling time is set to 0.002 [sec], and time delay L uses time of sampling interval.

Desired trajectory of TDC and ETDC is represented in figure B.1. Each desired trajectory is same

trajectory and the results are represented in figure B.2.

figure B.2, ETDC shows that range of tracking error reduced. However, ETDC shows the noise

including chattering.

	Joint 1	Joint 2	Joint 3	Joint 4	Joint 5	Joint 6
$\bar{M}$	0.0320	0.0280	0.0300	0.0300	0.0115	0.0062
K_D	20	20	20	20	20	20
K_P	100	100	100	100	100	100

Table B.1 Value of gains for TDC

	Joint 1	Joint 2	Joint 3	Joint 4	Joint 5	Joint 6
$\bar{M}$	0.00480	0.00410	0.00620	0.00420	0.00148	0.00075
K_D	20	20	20	20	20	20
K_P	100	100	100	100	100	100

Table B.2 Value of gains for ETDC
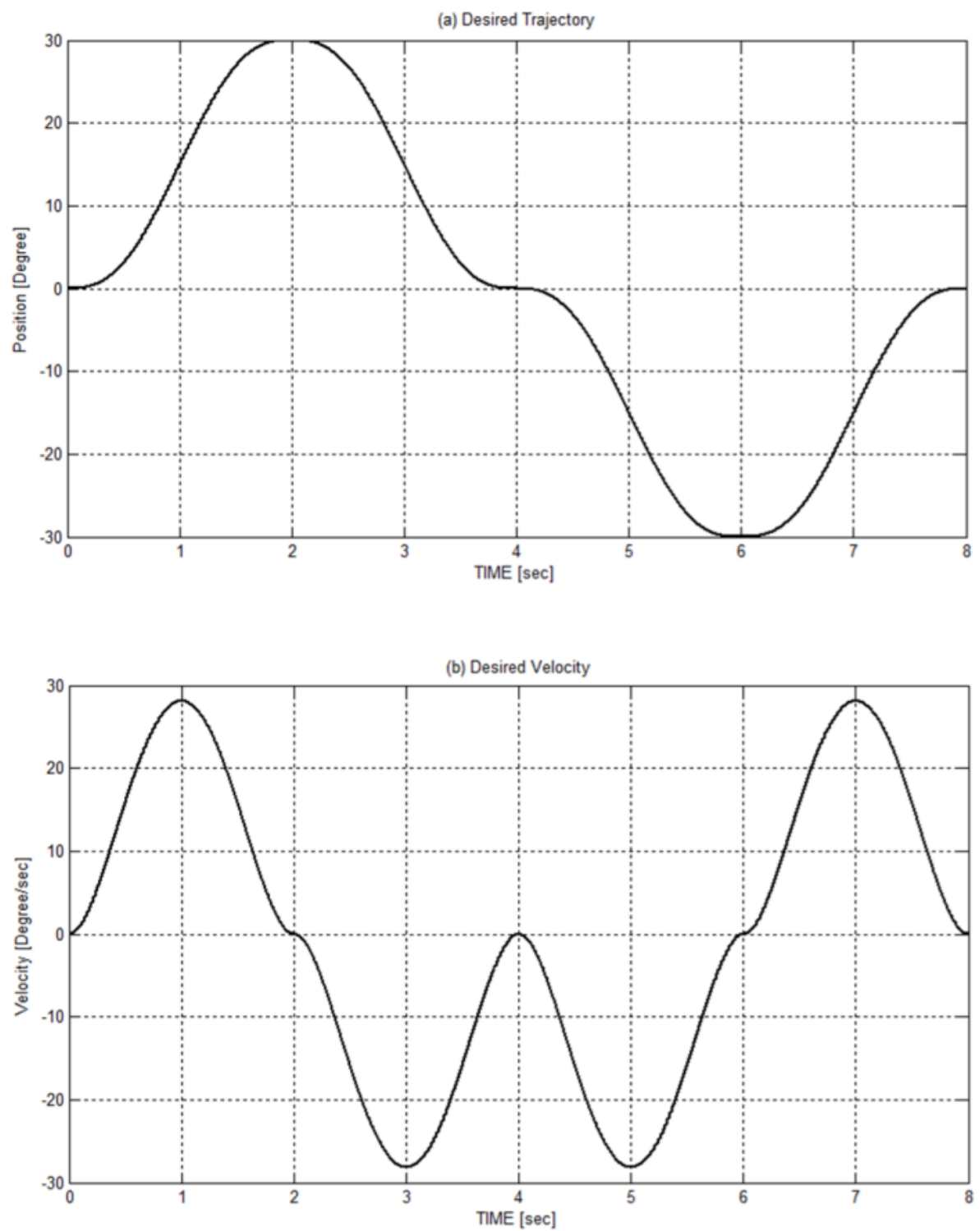
Fig. B.1 Desired input for appendix B: (a) desired trajectory (b) desired velocity
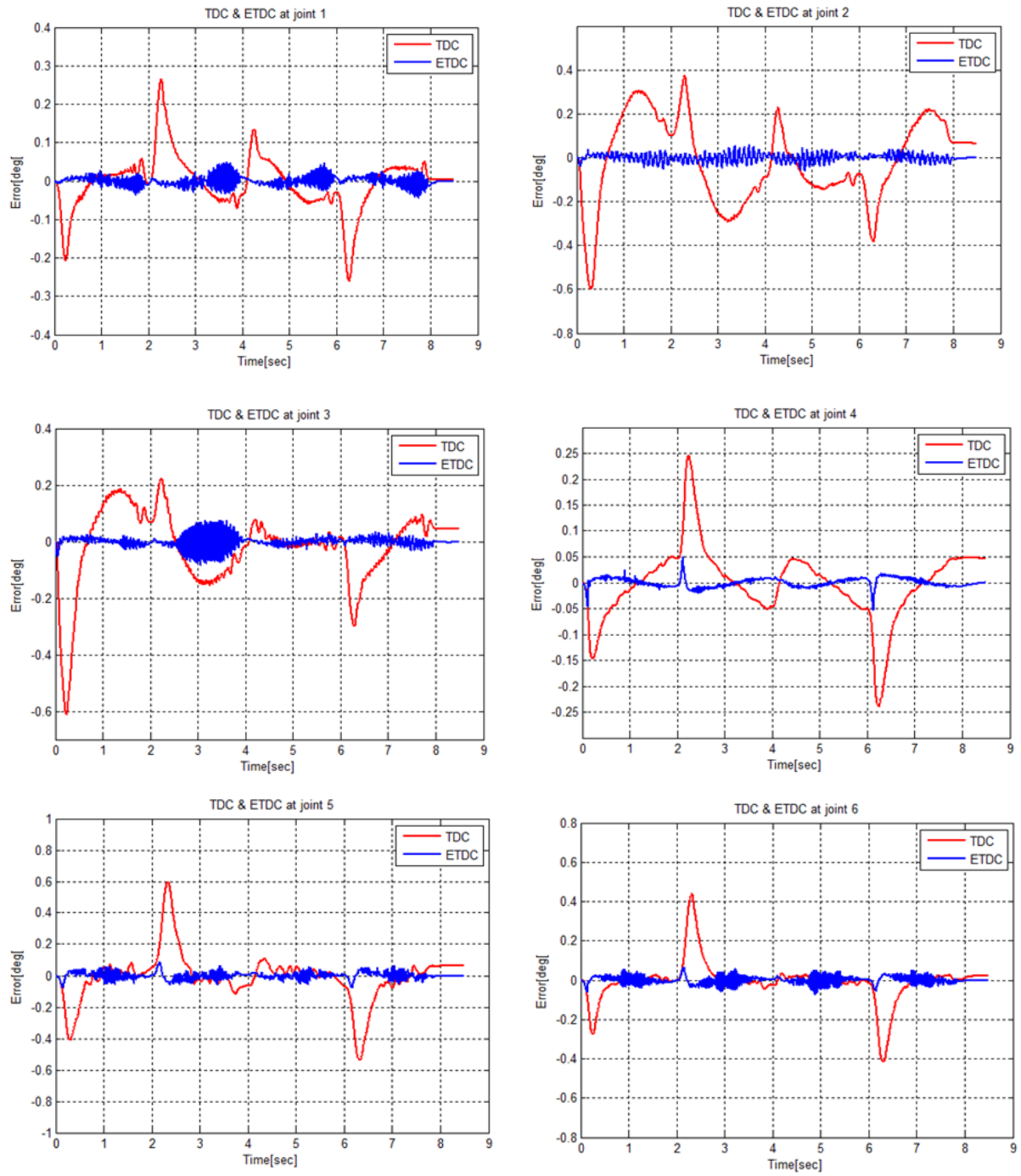
Fig. B.2 Tracking error of TDC and ETDC

요약문

로봇 매니퓰레이터를 위한 이차시간지연추정방법을
이용한 향상된 시간지연제어

로봇 매니퓰레이터는 매우 비선형적이며(highly nonlinear), 관절 별 동역학이 서로 강하게 연관된(strongly coupled)된 플랜트이다. 따라서, 로봇의 움직임을 정확히 제어하기 위해서는 매우 복잡한 비선형제어기가 필요하게 된다. 그러나 실제로 이런 제어기를 설계한다는 것은 어려울 뿐만 아니라, 제어기의 구현 측면에서도 비효율적이다. 따라서 좀 더 간단한 구조를 가지면서도 플랜트의 비선형성이나 외란(disturbance)에 강인한 제어기법이 요구 되었다.

이러한 요구에 부응할 수 있는 제어기법으로서 시간지연을 이용한 제어기법(Time Delay Control: TDC)이 제안되었다. TDC 는 플랜트의 예측 못한 외란이나 잘 모르는 비선형 동역학을 추정하기 위해 시간지연추정(Time Delay Estimation: TDE)을 이용하는 제어기이다. 이 제어기는 지금까지 개발된 고등 제어 알고리즘에 비하여 단순한 구조를 지니면서도, 외란과 매개변수의 변동에 대한 우수한 강인성을 보인다. 하지만, TDE 기법의 이용으로, 시간 지연된 입력과 출력을 이용하기 때문에, 시간지연 보다 빠른 동역학 특성, 소위 Hard Nonlinearity 로 분류되는 정지 마찰력(static friction)이나 쿨롱마찰력(coulomb friction)이 플랜트에 존재할 경우, TDC 의 제어 성능이 저하되는 현상을 보여준다. 이러한 시간지연추정 기법의 사용시, 생기는 시간지연추정 오차에 의해서 시간지연제어기의 성능을 저하시킨 것이다. 이 시간지연추정 오차를 보상하여 제어 성능을 더욱 향상시킨 제어기로는 향상된 시간지연제어(Enhanced Time Delay Control: ETDC)가 제안되었다. 향상된 시간지연제어기법은 전반적으로 시간지연제어기법에 비해, 좋은 성능을 보여준다. 하지만, 향상된 시간지연제어기법은 기존의 시간지연제어기법에 비해 채터링(chattering)같은 현상을 보여준다. 따라서 향상된 시간지연제어기법의 이러한 문제를 해결하기 위해, 이차 시간지연추정을 이용한 향상된 시간지연제어(Enhanced Time-Delay Control

using a Second-Order Time Delay Estimation)를 이 논문에서 제안한다. 제안한 제어기법은 시간지연제어기법과 향상된 시간지연제어기법의 중간 정도의 특성을 가지고 있다. 제안한 제어기법에서는 채터링과 같은 문제를 유발하지 않는 시간지연제어기법의 특성을 가지면서도, 향상된 시간지연제어기법의 뛰어난 제어성능을 보여준다.

 제안하는 제어기의 설계 방법은 기존의 향상된 시간지연 제어에서 사용한 시간지연추정 오차 보상항을 시간지연추정오차에 관하여 유도한 다음 그 유도된 시간지연추정오차 항과 어떠한 게인과 결합함으로써 설계 할 수 있다. 그 게인은 특성게인(characteristic gain)이라 명명 되었으며, 이 게인의 범위는 0 과 1 사의 값을 가진다. 이 게인이 0 으로 가깝게 설정이 되었을 때, 제안한 제어기의 특성은 기존의 시간지연제어기법과 가까운 특성을 보여준다. 하지만 그 게인값을 1 에 가깝게 설정을 할 경우, 제안한 제어기는 향상된 시간지연제어기법의 특성을 보여준다. 따라서 이 게인을 적절히 선정하여 제안한 제어기법을 적용하면, 기존의 시간지연제어기보다는 월등한 제어성능을 보여주면서, 향상된 시간지연제어기의 문제점인 채터링 문제점을 완화시킨 제어성능을 나타낸다. 이 제안한 제어기법은, 주파수응답특성해석을 통하여 실제로 기존의 시간지연제어기법과 향상된 시간지연제어기법의 특성을 가진 것을 증명한다. 1 자유도 로봇 매니퓰레이터와 2 자유도 매니퓰레이터의 시뮬레이션실험으로 향상된 시간지연제어기와 성능을 비교하였다. 또한, 실제 6 축 로봇실험을 통하여 제안한 제어기법의 특성을 보여주기 위한 실험과 더불어, 향상된 시간지연제어기법과 비교실험을 통하여 제안한 제어기법의 우수한 제어성능을 증명한다.

 핵심어: 시간지연제어(TDC), 시간지연추정(TDE), 시간지연추정 오차(TDE error),
        향상된 시간지연제어(ETDC), 채터링(chattering)

감사의 글

지인 및 대학교 선배님께 감사 드립니다. 나의 오랜 형님이신 한식이 형, 수덕이 형, 지훈이 형, 형호 형, 준혁이 형, 대성이 형, 태한이 형, 만길이 형, 정인이 형, 병우 형, 승환이 형, 지환이 형, 항목이 형, 창용이 형, 동규 형, 동환이 형, 성모 형 모두 감사합니다. 친구 및 대학교 후배님들에게도 감사 드립니다. 한상희, 우신이, 호상이, 한일이, 승덕이, 명성이, 홍록이, 방현이, 상래, 민욱이, 준민이, 연수, 은혜, 승환이, 우영이, 정민이, 인표, 우리 외 모든 분들에게 감사를 드립니다.

이 외에도 석사과정을 하면서 많은 이들의 도움을 알게 모르게 받았습니다. 다시 한번 모두에게 감사 드립니다. 이 논문은 하나의 논문일 뿐입니다. 하지만, 동시에 저의 인생에 있어서는 한 단계 더 성장할 수 있는 계기가 되었습니다. 미래에는 오늘보다 더 발전된 제가 있기를 바라며, 여러 방면으로 많은 도움 주신 모든 분들에게 진심으로 감사합니다.

Curriculum Vitae

Name　　　　: JinHo Do

Birth Date　　: July 31, 1985

Education

2011.3 ~ 2013. 8: Master of Robotics Engineering, Daegu Gyeongbuk Institute of Science and
Technology (DGIST), Korea

2003.3 ~ 2011. 2: Bachelor of Mechanical Engineering, Kumoh National Institute of Technology,
Korea.